

Symmetry induced enhancement in finite-time thermodynamic trade-off relations

Ken Funo

Department of Applied Physics, The University of Tokyo,
7-3-1 Hongo, Bunkyo-ku, Tokyo 113-8656, Japan*

Hiroyasu Tajima

Graduate School of Informatics and Engineering, The University of Electro-Communications,
1-5-1 Chofugaoka, Chofu, Tokyo 182-8585, Japan
(Dated: December 24, 2024)

Symmetry imposes constraints on open quantum systems, affecting the dissipative properties in nonequilibrium processes. Superradiance is a typical example in which the decay rate of the system is enhanced via a collective system-bath coupling that respects permutation symmetry. Such model has also been applied to heat engines. However, a generic framework that addresses the impact of symmetry in finite-time thermodynamics is not well established. Here, we show a symmetry-based framework that describes the fundamental limit of collective enhancement in finite-time thermodynamics. Specifically, we derive a general upper bound on the average jump rate, which quantifies the fundamental speed set by thermodynamic speed limits and trade-off relations. We identify the symmetry condition which achieves the obtained bound, and explicitly construct an open quantum system model that goes beyond the enhancement realized by the conventional superradiance model.

Introduction.— Symmetry plays a fundamental role in physics, as it provides a powerful tool to analyze, classify, and design the system of interest, and imposes constraints on physical systems such as superselection rules, charge conservations, and so forth. Realistic systems are unavoidably open to their surrounding degrees of freedom, and hence recent studies [1–6] aim to understand the impact of symmetry in open quantum systems. Consequently, discussions based on the symmetry of the Hamiltonian have been extended to those based on non-Hermitian Hamiltonians [7, 8] and Gorini-Kossakowski-Sudarshan-Lindblad (GKSL) master equations [9–11]. Symmetry is also related to topology [3–6], degeneracies [12], conserved quantities [2], decoherence-free subspaces, and noiseless subsystems [13], crucial for condensed matter physics and quantum information science.

Symmetry affects not only the equilibrium or steady-state properties of the system, but also the speed and dissipative properties in finite-time and nonequilibrium processes. When we consider permutation-invariant N identical two-level systems, the decay rate can be enhanced by a factor of N via collective system-bath coupling effects, termed superradiance [14, 15]. This example implies that symmetry is strongly connected to the notion of collective advantages, which have been extensively studied in the context of quantum thermodynamics, including setups such as heat engines [16–23], quantum batteries [24–26], information erasure protocols [27, 28], and photocells [29]. It is therefore expected that designing quantum devices that respect symmetry leads to the suppression of unwanted energetic costs, crucial for charge transport dynamics and quantum information processing

protocols. However, a general framework that addresses the influence of symmetry in finite-time and nonequilibrium thermodynamic processes has not been well established.

To develop a general theory to describe the impact of symmetry in finite-time thermodynamics, we pay attention to the thermodynamic speed limit inequalities [30–32] and trade-off relations [20, 33], which set generic upper bounds on the speed of state transformation and the change of the expectation values of physical quantities in open quantum systems. These relations indicate that increasing the average jump rate allows having smaller energetic costs (entropy production) while fixing the duration of the process (see Fig. 1). Therefore, investigation of symmetry in thermodynamic trade-off relations provides a unified approach to understanding collective advantages in quantum thermodynamics. Moreover, in view of the close relation between degeneracy and symmetry [12, 13], such investigation allows symmetry-based understanding of the effect of degeneracy and coherence on quantum thermodynamics [20].

In this Letter, we develop a generic framework describing the fundamental limit of symmetry-based enhancement in finite-time thermodynamics (see Fig. 1). Specifically, we derive a general upper bound on the average jump rate, showing that the number of degeneracy sets the maximum enhancement. We also derive the symmetry condition on the quantum state and the jump operators that saturates the obtained bound. As an application, we consider a permutation-invariant N two-level systems, and discuss the scaling behavior of the power and efficiency of heat engines, based on the power-efficiency trade-off relation [20]. The obtained theory predicts the possibility of realizing a heat engine that operates near the Carnot efficiency as $\eta = \eta_{\text{Car}} - O(1/N)$ while producing the power that scales from $O(N^2)$ to ex-

* funo@ap.t.u-tokyo.ac.jp

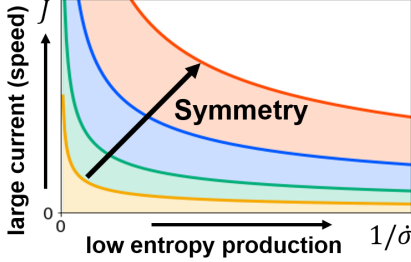


FIG. 1. Schematic picture of the current-dissipation trade-off relation $2J^2/\dot{\sigma} \leq A$ [20], where J is the heat current and $\dot{\sigma}$ is the entropy production rate. When the open system dynamics respects certain type of symmetry, the upper bound A can be enhanced (see Fig. 2)), and thus higher values of the ratio $J^2/\dot{\sigma}$ can be realized. We derive the fundamental limit of this enhancement [see Eq. (9)].

ponential, which goes beyond the scaling realized by the superradiant heat engine models [17, 18].

Setup.— We assume that the system of interest is interacting with a heat bath. The interaction Hamiltonian reads $H_{\text{int}} = \sum_a S_a \otimes B_a$, where S_a and B_a are Hermitian operators of the system and the bath, respectively. We describe the reduced dynamics of the system by considering a weak-coupling and Born-Markov-Secular approximations. Following the standard derivation under these conditions, we obtain the GKSL form of the master equation [9–11] (we take $\hbar = 1$)

$$\partial_t \rho = \mathcal{L} \rho = -i[H, \rho] + \sum_{a,\omega} \gamma_{a,\omega} \mathcal{D}[L_{a,\omega}] \rho, \quad (1)$$

where $\mathcal{D}[L]\rho = L\rho L^\dagger - (1/2)\{L^\dagger L, \rho\}$ is the dissipator, $\gamma_{a,\omega}$ is the decay rate, and $L_{a,\omega} = \sum_{\omega=\epsilon_k-\epsilon_l} \Pi_l S_a \Pi_k$ is the Lindblad jump operator that let the system jump from one energy eigenstate to another with their energy difference equal to ω . Here, Π_k is the projection to the k -th energy eigenspace \mathcal{S}_k , and ϵ_k is the k -th energy eigenvalue, i.e., $H = \sum_k \epsilon_k \Pi_k$. We denote $\mathcal{N}_k = \dim(\Pi_k)$ as the number of degeneracy of the k -th energy. We further assume the detailed balance condition $\gamma_{a,-\omega} = \gamma_{a,\omega} e^{-\beta\omega}$ to make Eq. (1) thermodynamically consistent, where β is the inverse temperature of the heat bath.

One of the main objectives in the field of stochastic thermodynamics is to minimize the entropy production in finite-time processes [34–38]. To this end, we focus on the activity [30, 39] $A_{\text{act}} = \sum_a A_\omega$ and an activity-like quantity $A = \sum_\omega \omega^2 A_\omega$, where

$$A_\omega(\rho, L_{a,\omega}) = \sum_a \gamma_{a,\omega} \text{Tr}[L_{a,\omega}^\dagger L_{a,\omega} \rho], \quad (2)$$

is the average jump rate with fixed transition energy ω . Note that these quantities set a time-scale of the system and play a fundamental role in stochastic thermodynamics. Specifically, the current-dissipation trade-off relation reads $2J^2/\dot{\sigma} \leq A$, where J is the heat current, $\dot{\sigma}$ is the en-

tropy production rate [20, 33, 40]. This trade-off bound is achievable in specific examples [20]. Therefore, suppressing the entropy production while producing a large heat current becomes possible when the value of A is increased (see Fig. 1).

Moreover, A_ω quantifies the transition rate from a k -th energy eigenstate $|\psi_k\rangle$ to a l -th energy eigenstate $|\psi_l\rangle$, given by $\sum_{a,\omega} \gamma_{a,\omega} |\langle \psi_l | L_{a,\omega} | \psi_k \rangle|^2 = A_{\epsilon_k - \epsilon_l} (|\psi_k\rangle \langle \psi_l|)$. Therefore, having a large A_ω allows increasing the emission of photons to the environment, with the possibility of realizing the enhancement that goes beyond superradiance.

Symmetry.— In what follows, we develop a symmetry-based theory that quantifies the limit of the enhancement of A_ω . To this end, we introduce a symmetry group G and assume that the Hamiltonian H is invariant under this group: $[H, V_g] = 0$ for all $g \in G$, where V_g is a unitary representation of the group. We then classify quantum states and jump operators based on V_g , which constitutes the core of our analysis. To this end, we assume in the main text that we take appropriate G and V_g whose precise condition is given in Appendix A, such that the symmetry represented by V_g perfectly characterizes the structure of the energy eigenspaces of H . Note that the examples that we discuss later satisfy this condition. On the other hand, the above condition is not satisfied when G does not represent all the symmetry of the Hamiltonian H , e.g., by choosing G as a trivial group, or by only choosing G as the permutation group for the permutation and even number bit-flip invariant system considered in *Example 2*. In Appendix B, we generalize our results to any choice of G and V_g . In particular, the main result (9) is still valid, but the bound is no longer achievable in general; we thus further derive an achievable bound on A_ω .

We point out that $A_\omega(\rho, L_{a,\omega}) = \sum_k p_k A_\omega(\rho_k, L_{a,\omega})$, where $p_k = \text{Tr}[\Pi_k \rho]$, and $\rho_k = \Pi_k \rho \Pi_k / p_k$. This relation motivates us to characterize quantum states ρ by their properties of ρ_k acting on \mathcal{S}_k . We now introduce following two special classes of quantum states based on V_g :

- *Local states* ρ_k^{loc} , defined by

$$\frac{1}{|G|} \sum_{g \in G} V_g \rho_k^{\text{loc}} V_g^\dagger = \frac{1}{\mathcal{N}_k} \Pi_k. \quad (3)$$

This definition means that by randomly mixing a local state by unitary operators V_g , it gets completely mixed and becomes the maximally mixed state in \mathcal{S}_k . We also introduce the local energy eigenbasis $\mathcal{B}_k^{\text{loc}} = \{|\psi_k^{\text{loc}}(\alpha)\rangle\}_{\alpha=1}^{\mathcal{N}_k}$ for \mathcal{S}_k , where each element of $\mathcal{B}_k^{\text{loc}}$ satisfies Eq. (3).

- *Symmetric states* ρ_k^{sym} , defined by

$$V_g \rho_k^{\text{sym}} = \rho_k^{\text{sym}} V_g^\dagger = \rho_k^{\text{sym}} \quad \text{for all } g. \quad (4)$$

This definition means that symmetric states do not

	local jump op. $\{L_{a,\omega}^{\text{loc}}\}$	sym. jump op. $\{L_{a,\omega}^{\text{sym}}\}$
local state ρ_k^{loc}	$c_k(L_{a,\omega}^{\text{loc}})$	$c_k(L_{a,\omega}^{\text{sym}})$ (no enhancement)
sym. state ρ_k^{sym}	$c_k(L_{a,\omega}^{\text{loc}})$ (no enhancement)	$\mathcal{N}_k c_k(L_{a,\omega}^{\text{sym}})$ (max. enhancement)

TABLE I. Classification of the enhancement of A_ω . If either the state or the jump operator is local, A_ω is given by c_k , and cannot be enhanced (7) and (8). If both the state and the jump operator are symmetric, A_ω is maximally enhanced, characterized by the number of degeneracy \mathcal{N}_k (9).

change by the action of V_g .

Next, we consider the symmetry-based classification of jump operators. To this end, we introduce the following covariant condition (so-called weak symmetry condition) for the Liouvillian $\mathcal{L}(V_g x V_g^\dagger) = V_g \mathcal{L}(x) V_g^\dagger$ for any operator x and for all $g \in G$ [1]. This condition imposes the Liouvillian \mathcal{L} to preserve symmetry. Now, we introduce two special types of the jump operators:

- *Local jump operators* $\{L_{a,\omega}^{\text{loc}}\}$, defined by

$$[(L_{a,\omega}^{\text{loc}})^\dagger L_{a,\omega}^{\text{loc}}, |\psi_k^{\text{loc}}(\alpha)\rangle\langle\psi_k^{\text{loc}}(\alpha)|] = 0 \text{ for all } \alpha. \quad (5)$$

Therefore, local jump operators do not create coherence between local states $|\psi_k^{\text{loc}}(\alpha)\rangle$ and $|\psi_k^{\text{loc}}(\alpha')\rangle$.

- *Symmetric jump operators* $\{L_{a,\omega}^{\text{sym}}\}$, defined by

$$V_g L_{a,\omega}^{\text{sym}} = L_{a,\omega}^{\text{sym}} V_g^\dagger = L_{a,\omega}^{\text{sym}} \text{ for all } g. \quad (6)$$

Similar to symmetric states, symmetric jump operator do not change by the action of V_g .

To see why we call $\{L_{a,\omega}^{\text{loc}}\}$ and $\{|\psi_k^{\text{loc}}(\alpha)\rangle\}$ as local, let us consider a permutation-invariant, N identical two-level systems discussed in *Example 1*. We then find that $|\psi_k^{\text{loc}}\rangle = |e\rangle^{\otimes k} \otimes |g\rangle^{\otimes N-k} \in \mathcal{B}_k^{\text{loc}}$, where $|g\rangle$ and $|e\rangle$ denote the ground and excited states of individual two-level systems. This state $|\psi_k^{\text{loc}}\rangle$ is “local” in the sense that it is a tensor product of individual two-level states, and does not have superpositions among different subsystems. We also note that the jump operators $\{\sigma_i^-\}_{i=1}^N$ satisfy Eq. (5), where σ_i^- is the lowering operator that acts “locally” on the i -th subsystem. With these in mind, we also call ρ_k^{loc} and $L_{a,\omega}^{\text{loc}}$ as local quantum states and local jump operators in generic situations.

In what follows, we utilize the above classification of the quantum states and jump operators and derive general properties of A_ω , including its upper bound.

No enhancement condition.— First, we show in the supplemental material [41] that

$$A_\omega(\rho^{\text{loc}}, \{L_{a,\omega}\}) = \sum_k p_k c_k(L_{a,\omega}), \quad (7)$$

$$A_\omega(\rho, \{L_{a,\omega}^{\text{loc}}\}) = \sum_k p_k c_k(L_{a,\omega}^{\text{loc}}), \quad (8)$$

where $c_k(L_{a,\omega}) = \mathcal{N}_k^{-1} \sum_a \gamma_{a,\omega} \text{Tr}[\Pi_k L_{a,\omega}^\dagger L_{a,\omega} \Pi_k]$ is the square of the Hilbert-Schmidt norm of the jump operators acting on the subspace \mathcal{S}_k divided by its dimension, and $\rho^{\text{loc}} = \sum_k p_k \rho_k^{\text{loc}}$. Note that if we consider a trivial rescaling $\sqrt{\gamma_{a,\omega}} L_{a,\omega} \rightarrow \sqrt{C \gamma_{a,\omega}} L_{a,\omega}$, the average jump rate is rescaled as $A_\omega \rightarrow C A_\omega$, where C is a constant. Therefore, it would be reasonable to analyze the amount of A_ω in units of some norm of the jump operators, and we have therefore introduced $c_k(L_{a,\omega})$. Equations (7) and (8) show that the norm of the jump operators $c_k(L_{a,\omega})$ sets the value of A_ω if at least one of the state and jump operator is local.

Maximum enhancement condition.— We now analyze, to what extent A_ω can be enhanced. In the supplemental material [41], we show a general upper bound on A_ω , for any density matrix ρ and jump operators $\{L_{a,\omega}\}$, expressed as

$$A_\omega(\rho, \{L_{a,\omega}\}) \leq \sum_k p_k \mathcal{N}_k c_k(L_{a,\omega}), \quad (9)$$

showing that A_ω can be enhanced up to \mathcal{N}_k times the norm of jump operators c_k for each k -th subspace. The equality condition in (9) is achieved by a combination of symmetric states and jump operators, given by

$$A_\omega(\rho^{\text{sym}}, \{L_{a,\omega}^{\text{sym}}\}) = \sum_k p_k \mathcal{N}_k c_k(L_{a,\omega}^{\text{sym}}), \quad (10)$$

where $\rho^{\text{sym}} = \sum_k p_k \rho_k^{\text{sym}}$. See Tab. I for the summary of the scaling of A_ω for different states and jump operators.

In what follows, we show specific examples and construct jump operators that realize better scaling of A_ω compared to the superradiance model. We also show that such jump operators allow enhancing the output power and efficiency of heat engines.

Example 1: permutation invariance.— We now apply our results to a permutation-invariant model. Let the system Hamiltonian be N identical two-level systems $H = (\omega_0/2) \sum_{i=1}^N \sigma_i^z$, where σ_i^z is the z -component of the Pauli matrix for the i -th system. This Hamiltonian is invariant under interchange of subsystem labels i , and is thus invariant under the permutation group S_N . One example of the local state is given by $|\psi_k^{\text{loc}}\rangle = |e\rangle^{\otimes k} \otimes |g\rangle^{\otimes N-k}$, representing the state with k “local” excitations of the two-level systems. On the other hand, the symmetric state $\rho_k^{\text{sym}} = |\psi_k^{\text{sym}}\rangle\langle\psi_k^{\text{sym}}|$ is given by the symmetric Dicke state $|\psi_k^{\text{sym}}\rangle = \mathcal{N}_k^{-1/2} \sum_g V_g |\psi_k^{\text{loc}}\rangle$, where $\mathcal{N}_k = N C_k$ is the number of degeneracy.

In what follows, we demonstrate the obtained results by explicitly calculating $A_{\omega_0}(\rho_k^{\text{sym}}, L_{a,\omega_0})$ for different jump operators L_{a,ω_0} that removes one excitation from the system. For mixed states $\rho^{\text{sym}} = \sum_k p_k \rho_k^{\text{sym}}$, the scaling of A_ω is simply given by the linear combination $\sum_k p_k A_{\omega_0}(\rho_k^{\text{sym}}, L_{a,\omega_0})$. Note that the case of adding one

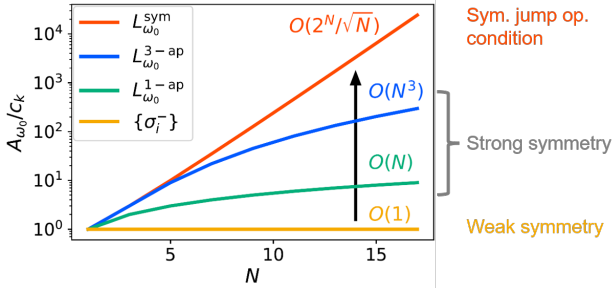


FIG. 2. Plot of $A_{\omega_0}(\rho_k^{\text{sym}}, L_{a,\omega_0})/c_k$ for a permutation-invariant N two-level systems model. We plot the case $k = \lceil N/2 \rceil$, i.e., half of the two-level systems are excited. The red curve is obtained by using the symmetric jump operator $L_{\omega_0}^{\text{sym}}$, demonstrating the optimal enhancement of A_{ω_0} . The blue curve is obtained by using $L_{\omega_0}^{\text{3-ap}}$, showing $O(N^3)$ scaling. The green curve is obtained by using the conventional collective jump operator $L_{\omega_0}^{\text{1-ap}} = \sum_i \sigma_i^-$ in the analysis of super-radiance, showing $O(N)$ scaling. The orange line is obtained by using local jump operators $\{\sigma_i^-\}$, demonstrating $A_{\omega_0}/c_k = 1$.

excitation to the system ($\omega = -\omega_0$) can be similarly obtained by using the jump operators $L_{a,-\omega_0} = L_{a,\omega_0}^\dagger$. In the following, we set $\gamma_{a,\omega_0} = \gamma_\downarrow$.

The symmetric jump operator (6) is given by

$$L_{\omega_0}^{\text{sym}} = \sum_{m=0}^{\lceil N/2 \rceil - 1} L_{\omega_0}^{(m)}, \quad (11)$$

where $L_{\omega_0}^{(m)} = \sum \sigma_{i_1}^- \cdots \sigma_{i_{m+1}}^- \sigma_{l_1}^+ \cdots \sigma_{l_m}^+$ and the summation is taken over $(i_1 < \cdots < i_{m+1}) \neq (l_1 < \cdots < l_m)$, and $\lceil \bullet \rceil$ is the ceiling function. We note that $L_{\omega_0}^{(m)}$ includes all possible combinations of $2m + 1$ -body jump operators that remove one excitation from the system. Using Eq. (11), we find that $A_{\omega_0}(\rho_k^{\text{sym}}, L_{\omega_0}^{\text{sym}}) = \mathcal{N}_k c_k$, with $c_k = N C_{k-1} \gamma_\downarrow$. When $k = \lceil N/2 \rceil$, we use Stirling's formula and obtain $\mathcal{N}_{N/2} \sim \sqrt{2/(\pi N)} 2^N$, showing an exponential scaling (see also Fig. 2).

Note that Eq. (11) consists of many-body system operators, which makes it challenging to realize the above optimal scaling in practice. In the following, we therefore approximate Eq. (11) by taking the first $2n + 1$ -body terms $L_{\omega_0}^{2n+1-\text{ap}} = \sum_{m=0}^n L_{\omega_0}^{(m)}$ and analyze the scaling of the average jump rate. In particular, the 1-body approximation reproduces the collective jump operator $L_{\omega_0}^{\text{1-ap}} = \sum_{i=1}^N \sigma_i^-$, which is used in the study of super-radiance [14]. The jump operator $L_{\omega_0}^{\text{1-ap}}$ satisfies strong symmetry [1] $[L_{\omega_0}^{\text{1-ap}}, V_g] = 0$, but does not satisfy Eq. (6). The scaling reads $A_{\omega_0}(\rho_k^{\text{sym}}, L_{\omega_0}^{\text{1-ap}}) = (N - k + 1)c_k$ with $c_k = k\gamma_\downarrow$. By considering the next order term $L_{\omega_0}^{3-\text{ap}}$, we find that $A_{\omega_0}(\rho_k^{\text{sym}}, L_{\omega_0}^{3-\text{ap}}) = (N - k + 1)[1 + (N - k)(k - 1)/2]c_k$, with $c_k = k(1 + (N - k)(k - 1)(k - 2)/2)\gamma_\downarrow$. When $k = \lceil N/2 \rceil$, A_{ω_0}/c_k scales $O(N^3)$, compared to the case of $O(N)$ scaling for the conventional superradiance model

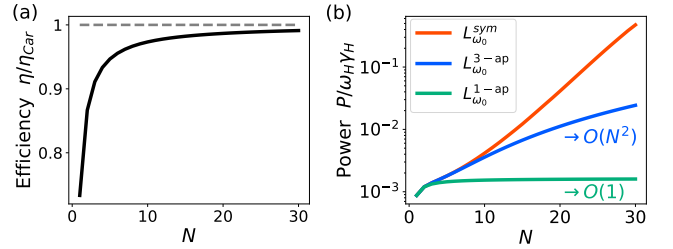


FIG. 3. Plot of the efficiency η/η_{Car} and the power $P/\omega_H \gamma_H$ of the permutation invariant N two-level system heat engine. (a) The efficiency (black curve) scales as $\eta = \eta_{\text{Car}} - b/N$ and asymptotically reaches the Carnot efficiency (gray dashed line). (b) By using the conventional superradiance model ($L_{\omega_0}^{\text{1-ap}}$), the power saturates at large N (green curve). If we use $L_{\omega_0}^{\text{3-ap}}$, the power scales $O(N^2)$ (blue curve), and if we use $L_{\omega_0}^{\text{sym}}$, the power scales exponentially (red curve). Here, ω_H and γ_H are the energy level splitting and the decay rate of the system during the hot thermalization stroke, respectively.

(see Fig. 2).

Finally, we consider local jump operators $\{\sigma_i^-\}_{i=1}^N$. This set of jump operators satisfies the weak symmetry, but does not satisfy the strong symmetry nor Eq. (6). We find that $A_{\omega_0} = c_k = k\gamma_\downarrow$, consistent with Eq. (8).

Application of Example 1 to heat engines.— We apply the permutation-invariant model to the analysis of heat engines. The output power P and the heat-to-work conversion efficiency η of the heat engines satisfy the power-efficiency trade-off relation [20, 33]

$$\frac{P}{\eta_{\text{Car}} - \eta} \leq c\bar{A}, \quad (12)$$

where $\eta_{\text{Car}} = 1 - \beta_H/\beta_C$ is the Carnot efficiency; β_H and β_C are the inverse temperatures of the hot and cold baths; $c = \beta_C \eta_{\text{Car}} / [2(2 - \eta_{\text{Car}})^2]$ is a constant; and $\bar{A} = \tau^{-1} \int_0^\tau dt \sum \omega^2 A_\omega$, where τ is the duration of time to complete one engine cycle.

We consider a finite-time quantum Otto heat engine using the jump operators $L_{\pm\omega_0}^{\text{1-ap}}$, $L_{\pm\omega_0}^{\text{3-ap}}$, and $L_{\pm\omega_0}^{\text{sym}}$ (see the supplementary material [41] for details). Because of the strong symmetry $[H, V_g] = [L_{a,\omega}, V_g] = 0$, if the initial state is prepared by $\rho^{\text{sym}}(0) = \sum_k p_k(0) \rho_k^{\text{sym}}$, the density matrix at later times remains in the same symmetric Dicke subspace spanned by $|\psi_k^{\text{sym}}\rangle$, and generically takes the form $\rho(t) = \sum_k p_k(t) \rho_k^{\text{sym}}$. Therefore, the scaling of A_ω discussed in the previous section can be directly applied to investigate the scalings of power and efficiency as follows (see also Appendix C).

We choose a protocol such that the efficiency asymptotically reaches the Carnot efficiency as $\eta = \eta_{\text{Car}} - b/N$, where b is a constant (see Fig. 3 (a)). In Fig. 3 (b), we show a numerical plot of the output power. The green curve shows the superradiant heat engine setup [17], where the jump operators are given by $L_{\pm\omega_0}^{\text{1-ap}}$. An analytical calculation shows $\bar{A} = O(N)$, and combined with Eq. (12), the power is expected to scale $O(1)$, which is

consistent with the numerical plot. If we instead consider $L_{\pm\omega_0}^{3\text{-ap}}$, a similar analysis implies that the power scales $O(N^2)$. By further considering $L_{\pm\omega_0}^{\text{sym}}$, we find an exponential scaling of the power (see Fig. 3).

Example 2: permutation and even bit flip invariance.— We next apply our results to a permutation and even number bit-flip (e.g., $V_g = \sigma_i^x \sigma_j^x$) invariant system. The Hamiltonian reads $H = \epsilon \prod_{i=1}^N \sigma_i^z$. When $N = 4$, this Hamiltonian appears in the Kitaev's toric code model as one of the stabilizer operators [42]. The eigenenergies and the number of degeneracies are given by $\pm\epsilon$ and $\mathcal{N}_{\pm\epsilon} = 2^{N-1}$, respectively. The symmetric state reads $|\psi_{\pm\epsilon}^{\text{sym}}\rangle = (|+\rangle^{\otimes N} \pm |-\rangle^{\otimes N})/\sqrt{2}$, where $|\pm\rangle = (|e\rangle \pm |g\rangle)/\sqrt{2}$. The symmetric jump operator reads

$$L_{2\epsilon}^{\text{sym}} = \sum_{m=0}^{[N/2]-1} \sum_{i_1 < \dots < i_{2m+1}} \Pi_{-\epsilon} \sigma_{i_1}^x \dots \sigma_{i_{2m+1}}^x \Pi_{\epsilon}. \quad (13)$$

Using Eq. (13), we obtain $A_{2\epsilon}(|\psi_{\epsilon}^{\text{sym}}\rangle\langle\psi_{\epsilon}^{\text{sym}}|, L_{2\epsilon}^{\text{sym}}) = \mathcal{N}_{\epsilon} c_{\epsilon}$ with $c_{\epsilon} = \mathcal{N}_{\epsilon} \gamma_{\downarrow}$, consistent with Eq. (10). This scaling behavior allows us to construct a heat engine model that achieves $\eta_{\text{Car}} - \eta = O(1/\mathcal{N}_{\epsilon})$ and $P = O(\mathcal{N}_{\epsilon})$ discussed in Ref. [20].

Conclusion.— We have shown that the number of degeneracy sets a general upper bound on the average jump rate, and derived a symmetry condition on the quantum states and jump operators that saturates the obtained bound. The obtained results clarify the effect of symmetry in finite-time thermodynamic trade-off relations. As an application, we consider a quantum heat engine composed of permutation invariant N two-level systems. In contrast to the conventional super-radiant heat engine model [17, 18], we obtained from $O(N^2)$ to exponential enhancement of the output power by designing the jump operators that better respects the obtained symmetry condition.

An interesting future direction is to generalize the obtained framework to generic situations, for example, when the detailed balance is violated [43], the system dynamics is generically non-Markovian [44, 45], and there are non-reciprocal interactions [46, 47]. The theoretical framework developed in this paper is anticipated to lead not only to designing high-performance heat engines but also to realizing fast and energy-efficient information processing devices and charge transport devices.

ACKNOWLEDGMENTS

Acknowledgements.— We thank Atsushi Noguchi for useful discussions. This work was supported by MEXT KAKENHI Grant-in-Aid for Transformative Research Areas B “Quantum Energy Innovation” Grant Nos. JP24H00830 and JP24H00831. K. F. acknowledges support from JSPS KAKENHI Grant No. JP23K13036 and JST ERATO Grant No. JPMJER2302, Japan. H.T. was supported by JST PRESTO No. JPMJPR2014, JST

MOONSHOT No. JPMJMS2061.

Appendix A: Details on the choice of G and V_g assumed in the main text

In this appendix, we show technical details on the appropriate choice of G and V_g assumed in the main text. We again note that the main result (9) can be generalized to arbitrary G and V_g , as shown in Appendix B.

To begin with, we note that the commutation relation $[V_g, H] = 0$ implies $[V_g, \Pi_k] = 0$. Then, V_g can be decomposed as $V_g = \bigoplus_k V_g^k$, where V_g^k acts on \mathcal{S}_k . Each V_g^k is further decomposed into irreducible representations as $V_g^k = \bigoplus_j I_{\mathcal{H}_j^k} \otimes \mathcal{V}_j^k(g)$, where \mathcal{S}_k is decomposed as $\mathcal{S}_k = \bigoplus_j \mathcal{H}_j^k \otimes \mathcal{K}_j^k$, $\mathcal{V}_j^k(g)$ is an irreducible representation of G acting on the subspace \mathcal{K}_j^k , $I_{\mathcal{H}_j^k}$ is the identity matrix acting on the subspace \mathcal{H}_j^k , and j labels irreducible representations [22, 48, 49]. Here, a representation $\mathcal{V}_j^k(g)$ of G acting on \mathcal{K}_j^k is called irreducible if \mathcal{K}_j^k has no nontrivial subspace that is invariant under the action of $\mathcal{V}_j^k(g)$ for all g . Therefore, the subspace \mathcal{H}_j^k is invariant under the operation of V_g^k , and \mathcal{K}_j^k is the only subspace in which V_g^k nontrivially acts on. When there exist (j, k) such that $\dim(\mathcal{H}_j^k) \geq 2$, the symmetry represented by V_g does not perfectly characterize the structure of the energy eigenspaces of H , due to these invariant subspaces. Fortunately, for a given H , we can always take appropriate G and V_g that satisfies $\dim(\mathcal{H}_j^k) = 1$ for any j and k (see the supplementary material [41]). We also note that the examples we discuss in the main text satisfy the condition $\dim(\mathcal{H}_j^k) = 1$ for any j and k for natural G and V_g . Therefore, in the main text, we assume that we take appropriate G and V_g that satisfy $\dim(\mathcal{H}_j^k) = 1$ for any j and k . In Appendix B, we discuss the case $\dim(\mathcal{H}_j^k) \geq 2$ and generalize the main results.

Appendix B: Generalization to arbitrary G and V_g

We now show how the main results are generalized to the case of $\dim(\mathcal{H}_j^k) \geq 2$, i.e., arbitrary G and V_g . To begin with, we introduce operators $\sigma_{j,k}$ and $B_{j,k}^{\omega}$ acting on the subspace \mathcal{H}_j^k to parametrize quantum states and jump operators as

$$[\rho_k]_{\text{inv}} = \frac{1}{\sum_j \text{Tr}[\sigma_{j,k}]} \bigoplus_j \sigma_{j,k} \otimes \frac{I_{\mathcal{K}_j^k}}{\dim(\mathcal{K}_j^k)}, \quad (14)$$

$$\left[\sum_a \gamma_{a,\omega} L_{a,\omega}^{\dagger} L_{a,\omega} \right]_{\text{inv}} = \bigoplus_{k,j} B_{j,k}^{\omega} \otimes \frac{I_{\mathcal{K}_j^k}}{\dim(\mathcal{K}_j^k)}, \quad (15)$$

where $[X]_{\text{inv}} := |G|^{-1} \sum_{g \in G} V_g X V_g^{\dagger}$. We again note that when $\dim(\mathcal{H}_j^k) \geq 2$, \mathcal{H}_j^k is a nontrivial invariant subspace under the action of V_g , and the specific form of $\sigma_{j,k}$ and $B_{j,k}^{\omega}$ cannot be constrained based on the symmetry conditions for given G and V_g . Nevertheless, a general upper bound on the average jump rate can be derived as (see

supplementary material [41] for details)

$$\begin{aligned} A_\omega(\rho, \{L_{a,\omega}\}) &\leq \sum_k p_k \mathcal{N}_k c_k(L_{a,\omega}) F(\sigma_{j,k}, B_{j,k}^\omega) \\ &\leq \sum_k p_k \mathcal{N}_k c_k(L_{a,\omega}), \end{aligned} \quad (16)$$

where

$$F(\sigma_{j,k}, B_{j,k}^\omega) = \frac{\sum_j \text{Tr}[\sigma_{j,k} B_{j,k}^\omega]}{\sum_j \text{Tr}[\sigma_{j,k}] \sum_j \text{Tr}[B_{j,k}^\omega]} \leq 1, \quad (17)$$

quantifies the overlap between $\{\sigma_{j,k}\}_j$ and $\{B_{j,k}^\omega\}_j$. The obtained relation (16) generalizes the result Eq. (9) to the case of $\dim(\mathcal{H}_j^k) \geq 2$. It should be noted that the bound (9) remains valid in this general case; however, the last equality condition in (16) can no longer be characterized by the properties of V_g . On the other hand, the first inequality in (16) is achievable by using symmetric states and jump operators (see supplementary material [41] for details)

$$A_\omega(\rho^{\text{sym}}, \{L_{a,\omega}^{\text{sym}}\}) = \sum_k p_k \mathcal{N}_k c_k(L_{a,\omega}^{\text{sym}}) F(\sigma_{j,k}^{\text{sym}}, B_{j,k}^{\text{sym},\omega}). \quad (18)$$

As shown in Eqs. (10) and (18), symmetric states and jump operators achieve the upper bound of the enhancement of A_ω . It should be noted that the existence of symmetric states and jump operators requires condition $\dim(\mathcal{K}_j^k) = 1$ for one j , which we denote as j_{sym} ; note that $\sigma_{j,k}^{\text{sym}} = B_{j,k}^{\text{sym},\omega} = 0$ for $j \neq j_{\text{sym}}$ is satisfied for symmetric states and jump operators. This condition $\dim(\mathcal{K}_{j_{\text{sym}}}^k) = 1$ is not necessarily satisfied for arbitrary G and V_g . Therefore, this condition $\dim(\mathcal{K}_{j_{\text{sym}}}^k) = 1$ can be viewed as a design principle of the Hamiltonian and jump operators to achieve the maximum enhancement of A_ω . Note that the examples that we discuss in the main text satisfy this condition. We also note that when $\dim(\mathcal{H}_j^k) = 1$, ρ_k^{sym} is unique (if it exists) and can be written as $\rho_k^{\text{sym}} = |\psi_k^{\text{sym}}\rangle\langle\psi_k^{\text{sym}}|$, where $|\psi_k^{\text{sym}}\rangle$ is defined by $V_g|\psi_k^{\text{sym}}\rangle = |\psi_k^{\text{sym}}\rangle$ for all g .

Appendix C: Scaling of A

Because the density matrix during a heat engine cycle is generically given by a mixed state, here we con-

sider the model discussed in Example 1 and show an additional plot that demonstrates the scaling of A for $\rho_{\text{th}}^{\text{sym}} = \sum_k p_k^{\text{th}} \rho_k^{\text{sym}}$, where $p_k^{\text{th}} = e^{-k\beta\omega_0} / \sum_{k=0}^N e^{-\beta k \omega_0}$ is the thermal occupation probability of the k -th energy eigenstate. Here, we consider the following master equation

$$\partial_t \rho = -i[H, \rho] + \gamma_\downarrow \mathcal{D}[L_{\omega_0}]\rho + \gamma_\uparrow \mathcal{D}[L_{\omega_0}^\dagger]\rho, \quad (19)$$

where $L_{\omega_0} = \{L_{\omega_0}^{1\text{-ap}}, L_{\omega_0}^{3\text{-ap}}, L_{\omega_0}^{\text{sym}}\}$, $L_{\omega_0}^\dagger = L_{-\omega_0}$, $\gamma_\downarrow = \Gamma_0/(1 + e^{-\beta\omega_0})$ and $\gamma_\uparrow = \Gamma_0/(1 + e^{\beta\omega_0})$ satisfy the detailed balance condition $\gamma_\downarrow/\gamma_\uparrow = e^{\beta\omega_0}$. Note that $\rho_{\text{th}}^{\text{sym}}$ is the steady-state of Eq. (19) when the initial

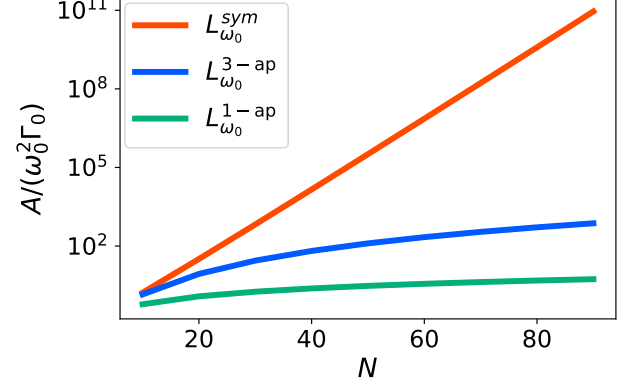


FIG. 4. Scaling of A for different jump operators when the density matrix is given by $\rho_{\text{th}}^{\text{sym}}$. The green curve is calculated by using $L_{\pm\omega_0}^{1\text{-ap}}$, the blue curve is calculated by using $L_{\pm\omega_0}^{3\text{-ap}}$, and the red curve is calculated by using $L_{\pm\omega_0}^{\text{sym}}$. See also the supplementary material [41] for further details of the scaling of A . The parameters are $\omega_0 = 0.7$, $\beta = 5$.

state is prepared in the symmetric Dicke subspace (e.g., $\rho^{\text{sym}}(0) = \sum_k p_k(0) \rho_k^{\text{sym}}$), because $L_{\pm\omega_0}^{1\text{-ap}}$, $L_{\pm\omega_0}^{3\text{-ap}}$, and $L_{\pm\omega_0}^{\text{sym}}$ satisfy the strong symmetry condition. In Fig. 5, we plot $A = \sum_{\omega=\pm\omega_0} \omega^2 A_\omega(\rho_{\text{th}}^{\text{sym}}, L_\omega)$, where its analytical expression, including the scaling of $A = O(N)$ for $L_{\pm\omega_0}^{1\text{-ap}}$ and $A = O(N^3)$ for $L_{\pm\omega_0}^{3\text{-ap}}$ is obtained in the supplementary material [41]. From Fig. 5, we also find that A scales exponentially for $L_{\pm\omega_0}^{\text{sym}}$.

Appendix A: Details on the setup and main results

1. Symmetry condition

Here, we summarize the symmetry condition on the jump operators introduced in the main text and show their relation. The master equation we consider is given by

$$\mathcal{L}\rho = -i[H, \rho] + \sum_{a,\omega} \gamma_{a,\omega} \left(L_{a,\omega} \rho L_{a,\omega}^\dagger - \frac{1}{2} \{L_{a,\omega}^\dagger L_{a,\omega}, \rho\} \right), \quad (\text{A1})$$

and the jump operators are given by

$$L_{a,\omega} = \sum_{\omega=\epsilon_k-\epsilon_l} \Pi_l S_a \Pi_k, \quad (\text{A2})$$

satisfying the relation $[\Pi_k, L_{a,\omega}^\dagger L_{a,\omega}] = 0$, where Π_k is the projection to the k -th energy eigenspace \mathcal{S}_k . We further assume the detailed balance condition $\gamma_{a,-\omega} = \gamma_{a,\omega} e^{-\beta\omega}$ to make Eq. (A1) thermodynamically consistent, where β is the inverse temperature of the heat bath.

We assume that the Hamiltonian is invariant under the symmetry group

$$[H, V_g] = 0 \text{ for all } g, \quad (\text{A3})$$

where V_g is a unitary representation of the group. Note that from Eq. (A3), it follows that

$$[\Pi_k, V_g] = 0 \text{ for all } g, \quad (\text{A4})$$

because for a given k -th energy eigenstate $|\psi_k\rangle$, the state $|\psi'_k\rangle = V_g|\psi_k\rangle$ is also a k -th energy eigenstate. In addition, we impose the weak symmetry condition (A7) on the jump operators. As we show below, the condition Eq. (A8) follows from Eqs. (A3) and (A7), and we shall mainly use the property of Eq. (A8) when deriving the main results.

Let us now summarize the conditions used in the main text and in the supplemental material as:

1. Symmetric jump operator condition

$$V_g L_{a,\omega} = L_{a,\omega} V_g^\dagger = L_{a,\omega} \text{ for all } g, \quad (\text{A5})$$

2. Strong symmetry [1]

$$[V_g, L_{a,\omega}] = 0 \text{ for all } g. \quad (\text{A6})$$

3. Weak symmetry [1]

$$\mathcal{L}(V_g x V_g^\dagger) = V_g \mathcal{L}(x) V_g^\dagger \text{ for any operator } x, \text{ and for all } g. \quad (\text{A7})$$

4. Symmetry condition

$$\left[\sum_a \gamma_{a,\omega} L_{a,\omega}^\dagger L_{a,\omega}, V_g \right] = 0 \text{ for all } \omega \neq 0, \text{ and for all } g. \quad (\text{A8})$$

By assuming Eq. (A3), these conditions satisfy Eq. (A5) \Rightarrow Eq. (A6) \Rightarrow Eq. (A7) \Rightarrow Eq. (A8).

Note that Eq. (A5) \Rightarrow Eq. (A6) is straightforward. To show Eq. (A6) \Rightarrow Eq. (A7), we use the condition on the Hamiltonian $[H, V_g] = 0$. Finally, we show Eq. (A7) \Rightarrow Eq. (A8). To this end, we introduce the adjoint of the Lindblad super operator \mathcal{L}^* by the relation $\langle A, \mathcal{L}(B) \rangle = \langle \mathcal{L}^*(A), B \rangle$, where $\langle A, B \rangle = \text{Tr}[A^\dagger B]$ is the Hilbert-Schmidt scalar product. The explicit form of \mathcal{L}^* is given by

$$\mathcal{L}^*(A) = i[H, A] + \sum_{a,\omega} \gamma_{a,\omega} \left(L_{a,\omega}^\dagger A L_{a,\omega} - \frac{1}{2} \{ L_{a,\omega}^\dagger L_{a,\omega}, A \} \right). \quad (\text{A9})$$

Using the weak symmetry condition (A7), we find that

$$\langle A, \mathcal{L}(V_g B V_g^\dagger) \rangle = \langle A, V_g \mathcal{L}(B) V_g^\dagger \rangle. \quad (\text{A10})$$

The left-hand side of Eq. (A10) can be further calculated as

$$\langle A, \mathcal{L}(V_g B V_g^\dagger) \rangle = \langle \mathcal{L}^*(A), V_g B V_g^\dagger \rangle = \langle V_g^\dagger \mathcal{L}^*(A) V_g, B \rangle. \quad (\text{A11})$$

Similarly, the right-hand side of Eq. (A10) can be further calculated as

$$\langle A, V_g \mathcal{L}(B) V_g^\dagger \rangle = \langle V_g^\dagger A V_g, \mathcal{L}(B) \rangle = \langle \mathcal{L}^*(V_g^\dagger A V_g), B \rangle. \quad (\text{A12})$$

By combining Eqs. (A10), (A11), and (A12), we obtain the corresponding symmetry condition on \mathcal{L}^* as

$$\mathcal{L}^*(V_g^\dagger x V_g) = V_g^\dagger \mathcal{L}^*(x) V_g \quad \text{for any operator } x, \text{ and for all } g. \quad (\text{A13})$$

Next, we use Eq. (A13) and obtain

$$\Pi_k \mathcal{L}^*(\Pi_l) \Pi_k = \Pi_k \mathcal{L}^*(V_g^\dagger \Pi_l V_g) \Pi_k = \Pi_k V_g^\dagger \mathcal{L}^*(\Pi_l) V_g \Pi_k. \quad (\text{A14})$$

By using Eqs. (A2) and (A9), the left-hand side of Eq. (A14) reads

$$\Pi_k \mathcal{L}^*(\Pi_l) \Pi_k = \sum_a \gamma_{a,\epsilon_k - \epsilon_l} L_{a,\epsilon_k - \epsilon_l}^\dagger L_{a,\epsilon_k - \epsilon_l} - \delta_{k,l} \Pi_k \sum_{a,\omega} \gamma_{a,\omega} L_{a,\omega}^\dagger L_{a,\omega} \Pi_k, \quad (\text{A15})$$

and the right-hand side of Eq. (A14) reads

$$\Pi_k V_g^\dagger \mathcal{L}^*(\Pi_l) V_g \Pi_k = V_g^\dagger \sum_a \gamma_{a,\epsilon_k - \epsilon_l} L_{a,\epsilon_k - \epsilon_l}^\dagger L_{a,\epsilon_k - \epsilon_l} V_g - \delta_{k,l} V_g^\dagger \Pi_k \sum_{a,\omega} \gamma_{a,\omega} L_{a,\omega}^\dagger L_{a,\omega} \Pi_k V_g. \quad (\text{A16})$$

By combining Eqs. (A14), (A15), and (A16) and by denoting $\omega = \epsilon_k - \epsilon_l$, we obtain

$$\sum_a \gamma_{a,\omega} L_{a,\omega}^\dagger L_{a,\omega} = V_g^\dagger \sum_a \gamma_{a,\omega} L_{a,\omega}^\dagger L_{a,\omega} V_g, \quad (\text{A17})$$

for $\omega \neq 0$, which shows Eq. (A8).

2. Irreducible decomposition

In this subsection, we give the irreducible decomposition of V_g discussed in the main text. First, from Eq. (A4), the unitary operator V_g can be decomposed as

$$V_g = \bigoplus_k V_g^k, \quad (\text{A18})$$

where each V_g^k acts on the k -th eigenspace \mathcal{S}_k . Now, each V_g^k can be decomposed into irreducible representations as

$$V_g^k = \bigoplus_j I_{\mathcal{H}_j^k} \otimes \mathcal{V}_j^k(g), \quad (\text{A19})$$

where $\mathcal{V}_j^k(g)$ is an irreducible representation of G acting on the subspace \mathcal{K}_j^k , $I_{\mathcal{H}_j^k}$ is the identity matrix acting on the subspace \mathcal{H}_j^k , and j labels irreducible representations. Here, the k -th energy eigenspace \mathcal{S}_k is decomposed as $\mathcal{S}_k = \bigoplus_j \mathcal{H}_j^k \otimes \mathcal{K}_j^k$, which means that the subspace \mathcal{H}_j^k is invariant under the operation of V_g^k , and \mathcal{K}_j^k is the only subspace in which V_g^k nontrivially acts on.

If $\dim(\mathcal{H}_j^k) \geq 2$, the chosen group G does not completely specify the symmetry of the Hamiltonian, in general. It is possible to construct unitary operators that nontrivially act on the subspace \mathcal{H}_j^k , which are related to unspecified groups G' (see, for example, Sec. E 1).

More generally, for given Hamiltonian H , group G , and its unitary representation V_g satisfying $[H, V_g] = 0$, we can appropriately choose a group G' and $\{\tilde{V}_{(g,g')}\}_{(g,g') \in G \times G'}$ such that $[\tilde{V}_{(g,g')}, H] = 0$ and the irreducible decomposition $\tilde{V}_{(g,g')} = \bigoplus_j I_{\tilde{\mathcal{H}}_j^k} \otimes \tilde{\mathcal{V}}_j^k(g, g')$ with $\dim(\tilde{\mathcal{H}}_j^k) = 1$ for any j, k is satisfied for $G \times G'$ and its unitary representation $\tilde{V}_{(g,g')}$, where $\tilde{\mathcal{V}}_j^k(g, g')$ acts on the subspace $\tilde{\mathcal{K}}_j^k$, and the k -th energy eigenspace is decomposed as $\mathcal{S}_k = \bigoplus_j \tilde{\mathcal{H}}_j^k \otimes \tilde{\mathcal{K}}_j^k$. To show this claim, start from the decomposition (A19). For each \mathcal{H}_j^k , we choose a group $G'_{(k,j)}$ and its unitary representation $\{U_{g'(k,j)}\}_{g'(k,j) \in G'_{(k,j)}}$, such that $U_{g'(k,j)}$ is an irreducible representation acting on \mathcal{H}_j^k ; for example, $SU(\dim(\mathcal{H}_j^k))$ and its natural representation satisfies this property. We then take $G' = \times_{(k,j)} G'_{(k,j)}$ and $\tilde{V}_{(g,g')} = \bigoplus_k \bigoplus_j U_{g'(k,j)} \otimes \mathcal{V}_j^k(g)$. We now note that because $U_{g'(k,j)}$ and $\mathcal{V}_j^k(g)$ are both irreducible, $U_{g'(k,j)} \otimes \mathcal{V}_j^k(g)$ is also an irreducible representation of $G \times G'_{(k,j)}$ acting on $\mathcal{H}_j^k \otimes \mathcal{K}_j^k$ [49]. Therefore, we have $\tilde{\mathcal{K}}_j^k = \mathcal{H}_j^k \otimes \mathcal{K}_j^k$ and thus $\dim(\tilde{\mathcal{H}}_j^k) = 1$. In summary, we can

always choose an appropriate group and its unitary representation that satisfies $\dim(\mathcal{H}_j^k) = 1$.

Because the subspace \mathcal{H}_j^k is invariant under the operation of V_g , we cannot constrain the form of the quantum states and jump operators within this invariant subspace by imposing conditions based on V_g . Specifically, there exists freedom in choosing the operators $\sigma_{j,k}$ and $B_{j,k}^\omega$ that act on the subspace \mathcal{H}_j^k as shown in Eqs. (B26) and (B27). By recalling that our main aim is to classify quantum states and jump operators based on V_g , we shall first consider the case of choosing an appropriate G and V_g and assume $\dim(\mathcal{H}_j^k) = 1$. We also discuss the general case $\dim(\mathcal{H}_j^k) \geq 2$ in Sec. B 5.

3. List of the local and symmetric states and jump operators

For clarity, let us list the definitions of local and symmetric states and jump operators introduced in the main text:

- Local states ρ_k^{loc} , defined by

$$\frac{1}{|G|} \sum_{g \in G} V_g \rho_k^{\text{loc}} V_g^\dagger = \frac{1}{\mathcal{N}_k} \Pi_k. \quad (\text{A20})$$

We also denote $\rho^{\text{loc}} = \sum_k p_k \rho_k^{\text{loc}}$, where p_k is the occupation probability of the k -th energy eigenstates.

- Local energy eigenbasis for \mathcal{S}_k , defined by

$$\mathcal{B}_k^{\text{loc}} = \{|\psi_k^{\text{loc}}(\alpha)\rangle\}_{\alpha=1}^{\mathcal{N}_k}, \quad (\text{A21})$$

where each element of $\mathcal{B}_k^{\text{loc}}$ satisfies Eq. (A20).

- Symmetric states

$$V_g \rho_k^{\text{sym}} = \rho_k^{\text{sym}} V_g^\dagger = \rho_k^{\text{sym}} \quad \text{for all } g. \quad (\text{A22})$$

- Local jump operators

$$[(L_{a,\omega}^{\text{loc}})^\dagger L_{a,\omega}^{\text{loc}}, |\psi_k^{\text{loc}}(\alpha)\rangle\langle\psi_k^{\text{loc}}(\alpha)|] = 0, \quad \text{for all } \alpha. \quad (\text{A23})$$

- Symmetric jump operators

$$V_g L_\omega^{\text{sym}} = L_\omega^{\text{sym}} V_g^\dagger = L_\omega^{\text{sym}} \quad \text{for all } g. \quad (\text{A24})$$

We note that the existence of symmetric states requires the condition $\dim(\mathcal{K}_j^k) = 1$ for one j . Otherwise, since $\mathcal{V}_j^k(g)$ nontrivially acts on the subspace \mathcal{K}_j^k , the condition (A22) cannot be satisfied. In the following, we denote the label j satisfying $\dim(\mathcal{K}_j^k) = 1$ as j_{sym} . Then, ρ_k^{sym} can be expressed as Eq. (B22). As noted in the main text, this condition is not necessarily satisfied for general G and V_g .

We note that local states and symmetric states are different in general. Suppose ρ_k satisfies both Eqs. (A20) and (A22). If we substitute Eq. (A22) into Eq. (A20), we find that $\rho_k = \Pi_k/\mathcal{N}_k$; however, this contradicts with Eq. (A22). Similarly, the conditions for local jump operators (B7) and symmetric jump operators (A24) cannot be satisfied simultaneously. Suppose L_ω satisfies Eqs. (B7) and (A24). From Eq. (B7), the jump operator takes the form $L_\omega^\dagger L_\omega = \sum_{k,\alpha} l_{k,\alpha}^\omega |\psi_k^{\text{loc}}(\alpha)\rangle\langle\psi_k^{\text{loc}}(\alpha)|$, where $l_{k,\alpha}^\omega$ is some coefficient. Then, by using Eq. (A24), we find that $L_\omega^\dagger L_\omega = |G|^{-1} \sum_g V_g \sum_{k,\alpha} l_{k,\alpha}^\omega |\psi_k^{\text{loc}}(\alpha)\rangle\langle\psi_k^{\text{loc}}(\alpha)| V_g^\dagger = \sum_k (\sum_\alpha l_{k,\alpha}^\omega) \Pi_k/\mathcal{N}_k$, but this contradicts with Eq. (A24).

Appendix B: Derivation of the main results

In this section, we show the main results Eqs. (7) to (10) presented in the main text. As discussed in the main text, we assume $\dim(\mathcal{H}_j^k) = 1$ from Sec. B 1 to Sec. B 4. We show the case of $\dim(\mathcal{H}_j^k) \geq 2$ in Sec. B 5, and discuss how the main results get modified by this generalization.

Because our main focus is on the scaling of the activity-like quantity $A = \sum_{\omega \neq 0} \omega^2 A_\omega$, we discuss the scaling of A_ω for $\omega \neq 0$ in the following.

We also note that, as it is apparent from the derivation given below, the main results Eqs. (7) to (10) do not rely on the detailed balance condition $\gamma_{a,-\omega} = \gamma_{a,\omega} e^{-\beta\omega}$; however, this condition is typically assumed in the (quantum) thermodynamics settings and is also assumed in the derivation of the current-dissipation trade-off relation $2J^2/\sigma \leq A$ [20]. Therefore, we shall assume the detailed balance condition throughout the paper.

1. A_ω for local states

We show Eq. (7) in the main text:

$$A_\omega(\rho^{\text{loc}}, \{L_{a,\omega}\}) = \sum_k p_k c_k(L_{a,\omega}). \quad (\text{B1})$$

We first note that

$$A_\omega(\rho^{\text{loc}}, \{L_{a,\omega}\}) = \sum_k p_k \text{Tr} \left[\sum_a \gamma_{a,\omega} L_{a,\omega}^\dagger L_{a,\omega} \rho_k^{\text{loc}} \right] = \sum_k p_k \text{Tr} \left[V_g^\dagger \sum_a \gamma_{a,\omega} L_{a,\omega}^\dagger L_{a,\omega} V_g \rho_k^{\text{loc}} \right], \quad (\text{B2})$$

where we use Eq. (A8) and obtain the second equality. Using the cyclic property of the trace and taking summation over g , we obtain

$$\begin{aligned} A_\omega(\rho^{\text{loc}}, \{L_{a,\omega}\}) &= \sum_k p_k \text{Tr} \left[\sum_a \gamma_{a,\omega} L_{a,\omega}^\dagger L_{a,\omega} \frac{1}{|G|} \sum_{g \in G} V_g \rho_k^{\text{loc}} V_g^\dagger \right] \\ &= \sum_k p_k \frac{1}{N_k} \text{Tr} \left[\sum_a \gamma_{a,\omega} L_{a,\omega}^\dagger L_{a,\omega} \Pi_k \right] = \sum_k p_k c_k(L_{a,\omega}), \end{aligned} \quad (\text{B3})$$

where we use Eq. (A20) and obtain the second line. Therefore, Eq. (B1) is obtained.

2. A_ω for local jump operators

We next show Eq. (8) in the main text:

$$A_\omega(\rho, \{L_{a,\omega}^{\text{loc}}\}) = \sum_k p_k c_k(L_{a,\omega}^{\text{loc}}). \quad (\text{B4})$$

To show Eq. (B4), we first show that the local jump operators $\{L_{a,\omega}^{\text{loc}}\}$ satisfy the following relation

$$\sum_a \gamma_{a,\omega} (L_{a,\omega}^{\text{loc}})^\dagger L_{a,\omega}^{\text{loc}} = \sum_k c_k(L_{a,\omega}^{\text{loc}}) \Pi_k \quad (\text{B5})$$

for $\omega \neq 0$, because by assuming Eq. (B5), we have

$$A_\omega(\rho, \{L_{a,\omega}^{\text{loc}}\}) = \sum_k p_k \text{Tr} \left[\sum_a \gamma_{a,\omega} (L_{a,\omega}^{\text{loc}})^\dagger L_{a,\omega}^{\text{loc}} \rho_k \right] = \sum_k p_k c_k(L_{a,\omega}^{\text{loc}}) \text{Tr}[\rho_k \Pi_k] = \sum_k p_k c_k(L_{a,\omega}^{\text{loc}}), \quad (\text{B6})$$

and Eq. (B4) can be obtained. Therefore, in what follows, we show Eq. (B5).

To show Eq. (B5), we take summation over a on both hand sides of the definition of the local jump operators (B7):

$$\left[\sum_a (L_{a,\omega}^{\text{loc}})^\dagger L_{a,\omega}^{\text{loc}}, |\psi_k^{\text{loc}}(\alpha)\rangle\langle\psi_k^{\text{loc}}(\alpha)| \right] = 0, \text{ for all } \alpha. \quad (\text{B7})$$

From the above relation, we have

$$\sum_a \gamma_{a,\omega} (L_{a,\omega}^{\text{loc}})^\dagger L_{a,\omega}^{\text{loc}} = \sum_k \sum_\alpha A_k^\alpha |\psi_k^{\text{loc}}(\alpha)\rangle\langle\psi_k^{\text{loc}}(\alpha)|, \quad (\text{B8})$$

where A_k^α is some coefficient. Using the commutation relation for jump operators Eq. (A8), we have

$$\sum_a \gamma_{a,\omega} (L_{a,\omega}^{\text{loc}})^\dagger L_{a,\omega}^{\text{loc}} = \frac{1}{|G|} \sum_{g \in G} V_g \left(\sum_a \gamma_{a,\omega} (L_{a,\omega}^{\text{loc}})^\dagger L_{a,\omega}^{\text{loc}} \right) V_g^\dagger = \frac{1}{|G|} \sum_{g \in G} V_g \sum_k \sum_\alpha A_k^\alpha |\psi_k^{\text{loc}}(\alpha)\rangle \langle \psi_k^{\text{loc}}(\alpha)| V_g^\dagger. \quad (\text{B9})$$

We then use the relation (A20) for local states

$$\frac{1}{|G|} \sum_{g \in G} V_g |\psi_k^{\text{loc}}(\alpha)\rangle \langle \psi_k^{\text{loc}}(\alpha)| V_g^\dagger = \frac{1}{\mathcal{N}_k} \Pi_k, \quad (\text{B10})$$

and obtain

$$\sum_a \gamma_{a,\omega} (L_{a,\omega}^{\text{loc}})^\dagger L_{a,\omega}^{\text{loc}} = \sum_k \sum_\alpha A_k^\alpha \frac{1}{\mathcal{N}_k} \Pi_k. \quad (\text{B11})$$

We further note that

$$c_k(L_{a,\omega}^{\text{loc}}) = \frac{1}{\mathcal{N}_k} \sum_a \gamma_{a,\omega} \text{Tr}[\Pi_k (L_{a,\omega}^{\text{loc}})^\dagger L_{a,\omega}^{\text{loc}} \Pi_k] = \sum_\alpha A_k^\alpha \frac{1}{\mathcal{N}_k^2} \text{Tr}[\Pi_k] = \frac{1}{\mathcal{N}_k} \sum_\alpha A_k^\alpha, \quad (\text{B12})$$

and by substituting Eq. (B12) into Eq. (B11) shows Eq. (B5).

3. General upper bound of A_ω

We now show a general upper bound on A_ω (Eq. (9) in the main text):

$$A_\omega(\rho, L_{a,\omega}) \leq \sum_k p_k \mathcal{N}_k c_k(L_{a,\omega}), \quad (\text{B13})$$

for any states ρ and any jump operators $L_{a,\omega}$.

To show Eq. (B13), we first note that

$$\begin{aligned} A_\omega(\rho, \{L_{a,\omega}\}) &= \sum_k p_k \text{Tr} \left[\sum_a \gamma_{a,\omega} L_{a,\omega}^\dagger L_{a,\omega} \rho_k \right] \\ &= \sum_k p_k \text{Tr} \left[V_g^\dagger \sum_a \gamma_{a,\omega} L_{a,\omega}^\dagger L_{a,\omega} V_g \rho_k \right] \\ &= \sum_k p_k \text{Tr} \left[\sum_a \gamma_{a,\omega} L_{a,\omega}^\dagger L_{a,\omega} \frac{1}{|G|} \sum_{g \in G} V_g \rho_k V_g^\dagger \right], \end{aligned} \quad (\text{B14})$$

where the second equality is obtained by using the commutation relation (A8). Because the density matrix $\frac{1}{|G|} \sum_{g \in G} V_g \rho_k V_g^\dagger$ commutes with V_g , we can express it using the block-diagonal form based on the irreducible decomposition (A19), which now reads

$$\frac{1}{|G|} \sum_{g \in G} V_g \rho_k V_g^\dagger = \frac{1}{\sum_j q_{j,k}} \bigoplus_j q_{j,k} |j, k\rangle \langle j, k| \otimes \frac{I_{\mathcal{K}_j^k}}{d_j^k}, \quad (\text{B15})$$

where we use $\dim(\mathcal{H}_j^k) = 1$ and denote the basis in \mathcal{H}_j^k as $|j, k\rangle$, $q_{j,k}$ is a coefficient, and $d_j^k = \dim(\mathcal{K}_j^k)$.

Similarly, the jump operators satisfy the commutation relation (A8), and can be block-diagonalized as

$$\sum_a \gamma_{a,\omega} L_{a,\omega}^\dagger L_{a,\omega} = \bigoplus_{k,j} b_{j,k}^\omega |j, k\rangle \langle j, k| \otimes \frac{I_{\mathcal{K}_j^k}}{d_j^k}, \quad (\text{B16})$$

where $b_{j,k}^\omega$ is a coefficient.

Using Eqs. (B15) and (B16), A_ω can be expressed as

$$A_\omega(\rho, \{L_{a,\omega}\}) = \sum_k p_k \frac{\sum_j (d_j^k)^{-1} q_{j,k} b_{j,k}^\omega}{\sum_j q_{j,k}} \leq \sum_k p_k \frac{\sum_j q_{j,k} b_{j,k}^\omega}{\sum_j q_{j,k}} \leq \sum_k p_k \sum_j b_{j,k}^\omega, \quad (\text{B17})$$

where the second inequality follows from

$$(d_j^k)^{-1} \leq 1 \text{ for all } j, \quad (\text{B18})$$

and the last inequality follows from

$$\frac{q_{j,k}}{\sum_j q_{j,k}} \leq 1 \text{ for all } j. \quad (\text{B19})$$

Finally, we note that

$$c_k(L_{a,\omega}) = \frac{1}{\mathcal{N}_k} \text{Tr} \left[\sum_a \gamma_{a,\omega} L_{a,\omega}^\dagger L_{a,\omega} \Pi_k \right] = \frac{1}{\mathcal{N}_k} \sum_j b_{j,k}^\omega. \quad (\text{B20})$$

By combining Eqs. (B17) and (B20), we obtain the main result (B13).

4. A_ω for symmetric state and jump operator

We now show that by using the symmetric states ρ^{sym} and jump operators $\{L_{a,\omega}^{\text{sym}}\}$, A_ω is given by Eq. (10) in the main text:

$$\mathcal{A}_\omega(\rho^{\text{sym}}, L_{a,\omega}^{\text{sym}}) = \sum_k p_k \mathcal{N}_k c_k(L_{a,\omega}^{\text{sym}}). \quad (\text{B21})$$

To show Eq. (B21), we start from the conditions (A22) and (A24), and express the symmetric state ρ_k^{sym} and jump operator $L_{a,\omega}^{\text{sym}}$ as

$$\rho_k^{\text{sym}} = |j_{\text{sym}}, k\rangle \langle j_{\text{sym}}, k| \otimes I_{\mathcal{K}_{j_{\text{sym}}}^k}, \quad (\text{B22})$$

$$\sum_a \gamma_{a,\omega}(L_{a,\omega}^{\text{sym}})^\dagger L_{a,\omega}^{\text{sym}} = \bigoplus_k b_{j_{\text{sym}},k}^\omega |j_{\text{sym}}, k\rangle \langle j_{\text{sym}}, k| \otimes I_{\mathcal{K}_{j_{\text{sym}}}^k}, \quad (\text{B23})$$

where $d_{j_{\text{sym}}}^k = \dim(\mathcal{K}_{j_{\text{sym}}}^k) = 1$. A direct calculation reads to

$$A_\omega(\rho^{\text{sym}}, L_{a,\omega}^{\text{sym}}) = \sum_k p_k b_{j_{\text{sym}},k}^\omega. \quad (\text{B24})$$

Combining Eq. (B24) with

$$c_k(L_{a,\omega}^{\text{sym}}) = \frac{1}{\mathcal{N}_k} b_{j_{\text{sym}},k}^\omega \quad (\text{B25})$$

shows the result (B21). We further note that because $q_{j_{\text{sym}},k} = 1$, $q_{j,k} = 0$ for $j \neq j_{\text{sym}}$, and $d_{j_{\text{sym}}}^k = 1$, the equality conditions in Eqs. (B18) and (B19) are satisfied, and thus the upper bound of (B13) is achieved.

5. The case when $\dim(\mathcal{H}_j^k) \geq 2$

Finally, we discuss how the results presented in the main text is modified when invariant subspace under the action of V_g^k exists, i.e., $\dim(\mathcal{H}_j^k) \geq 2$. The main results Eqs. (9) and (10) are now generalized to Eqs. (B30) and (B35), respectively.

We start by using Eq. (B14), since it is still valid when $\dim(\mathcal{H}_j^k) \geq 2$. However, Eqs. (B15) and (B16) get modified

as follows:

$$\frac{1}{|G|} \sum_{g \in G} V_g \rho_k V_g^\dagger = \frac{1}{\sum_j \text{Tr}[\sigma_{j,k}]} \bigoplus_j \sigma_{j,k} \otimes \frac{I_{\mathcal{K}_j^k}}{d_j^k}, \quad (\text{B26})$$

$$\sum_a \gamma_{a,\omega} L_{a,\omega}^\dagger L_{a,\omega} = \bigoplus_{k,j} B_{j,k}^\omega \otimes \frac{I_{\mathcal{K}_j^k}}{d_j^k}, \quad (\text{B27})$$

where $\sigma_{j,k}$ and $B_{j,k}^\omega$ are operators acting on the subspace \mathcal{H}_j^k . Using the expressions (B26) and (B27), we obtain

$$A_\omega(\rho, \{L_{a,\omega}\}) = \sum_k p_k \frac{\sum_j (d_j^k)^{-1} \text{Tr}[\sigma_{j,k} B_{j,k}^\omega]}{\sum_j \text{Tr}[\sigma_{j,k}]} \leq \sum_k p_k \frac{\sum_j \text{Tr}[\sigma_{j,k} B_{j,k}^\omega]}{\sum_j \text{Tr}[\sigma_{j,k}]}, \quad (\text{B28})$$

where we use the inequality (B18) and obtain the second inequality. We further note that

$$c_k(L_{a,\omega}) = \frac{1}{\mathcal{N}_k} \sum_j \text{Tr}[B_{j,k}^\omega]. \quad (\text{B29})$$

Combining Eqs. (B28) and (B29) gives an upper bound on the average jump rate

$$A_\omega(\rho, \{L_{a,\omega}\}) \leq \sum_k p_k \mathcal{N}_k c_k(L_{a,\omega}) \frac{\sum_j \text{Tr}[\sigma_{j,k} B_{j,k}^\omega]}{\sum_j \text{Tr}[\sigma_{j,k}] \sum_j \text{Tr}[B_{j,k}^\omega]} \quad (\text{B30})$$

$$\leq \sum_k p_k \mathcal{N}_k c_k(L_{a,\omega}), \quad (\text{B31})$$

which generalizes the result Eq. (9) to the case of $\dim(\mathcal{H}_j^k) \geq 2$. Note that the last inequality (B31) is obtained by noting that

$$\frac{\sum_j \text{Tr}[\sigma_{j,k} B_{j,k}^\omega]}{\sum_j \text{Tr}[\sigma_{j,k}] \sum_j \text{Tr}[B_{j,k}^\omega]} \leq 1, \quad (\text{B32})$$

and thus the equality condition in Eq. (B31) requires specific conditions on the form of $\sigma_{j,k}$ and $B_{j,k}^\omega$. However, the subspace \mathcal{H}_j^k is invariant under V_g^k , which means that one cannot characterize the equality condition in Eq. (B31) by using the properties of V_g^k . Therefore, the upper bound generically depends on the specific form of $\sigma_{j,k}$ and $B_{j,k}^\omega$, shown by the tighter inequality (B30).

Next, we show that the equality condition of (B30) can be achieved by using the symmetric states and jump operators. From the conditions (A22) and (A24), the symmetric state ρ_k^{sym} and jump operators $L_{a,\omega}^{\text{sym}}$ take the form

$$\rho_k^{\text{sym}} = \frac{1}{\text{Tr}[\sigma_{j_{\text{sym}},k}]} \sigma_{j_{\text{sym}},k} \otimes I_{\mathcal{K}_{j_{\text{sym}}}^k} \quad (\text{B33})$$

$$\sum_a \gamma_{a,\omega} (L_{a,\omega}^{\text{sym}})^\dagger L_{a,\omega}^{\text{sym}} = \bigoplus_k B_{j_{\text{sym}},k}^\omega \otimes I_{\mathcal{K}_{j_{\text{sym}}}^k}, \quad (\text{B34})$$

where $d_{j_{\text{sym}}}^k = \dim(\mathcal{K}_{j_{\text{sym}}}^k) = 1$. Note that depending on the freedom of the choice of $\sigma_{j_{\text{sym}},k}$, there could be multiple symmetric states. A direct calculation reads to

$$A_\omega(\rho^{\text{sym}}, L_{a,\omega}^{\text{sym}}) = \sum_k p_k \frac{\text{Tr}[\sigma_{j_{\text{sym}},k} B_{j_{\text{sym}},k}^\omega]}{\text{Tr}[\sigma_{j_{\text{sym}},k}]} = \sum_k p_k \mathcal{N}_k c_k(L_{a,\omega}^{\text{sym}}) \frac{\text{Tr}[\sigma_{j_{\text{sym}},k} B_{j_{\text{sym}},k}^\omega]}{\text{Tr}[\sigma_{j_{\text{sym}},k}] \text{Tr}[B_{j_{\text{sym}},k}^\omega]}, \quad (\text{B35})$$

by noting that

$$c_k(L_{a,\omega}^{\text{sym}}) = \frac{1}{\mathcal{N}_k} \text{Tr}[B_{j_{\text{sym}},k}^\omega]. \quad (\text{B36})$$

Therefore, the upper bound in (B30) is achieved by noting that $\sigma_{j,k} = B_{j,k}^\omega = 0$ for $j \neq j_{\text{sym}}$, and the equality

condition in (B18) is achieved since $d_{j_{\text{sym}}}^k = 1$. Therefore, the enhancement of A_ω for symmetric states and jump operators presented in Eq. (10) is generalized to Eq. (B35) when $\dim(\mathcal{H}_j^k) \geq 2$, as it depends on specific forms of $\sigma_{j_{\text{sym}},k}$ and $B_{j_{\text{sym}},k}^\omega$.

Appendix C: Details on the permutaiton-invariant two-level systems

In this section, we give further details on the identical two-level systems.

1. Permutation symmetry and block-diagonal structures

The Hamiltonian of the system is given by

$$H = \hbar\omega \sum_i^N \sigma_i^z, \quad (\text{C1})$$

which is permutation-invariant. By denoting the permutation group as S_N and a unitary representation of the group as V_g ($g \in S_N$), the Hamiltonian satisfies $[H, V_g] = 0$. Then, the k -th eigenspace is decomposed as

$$\mathcal{S}_k = \bigoplus_{j=|j_{\text{sym}}-k|}^{j_{\text{sym}}} \mathcal{H}_j^k \otimes \mathcal{K}_j^k, \quad (\text{C2})$$

where j labels the irreducible representation of S_N , $j_{\text{sym}} = N/2$, and $k = 0, \dots, N$. The projection operator Π_k , which satisfies $[\Pi_k, V_g] = [\Pi_k, V_g^k] = 0$ with $V_g = \bigoplus_k V_g^k$, can be decomposed as

$$\Pi_k = \bigoplus_{j=|j_{\text{sym}}-k|}^{j_{\text{sym}}} |j, k\rangle\langle j, k| \otimes I_{\mathcal{K}_j^k}, \quad (\text{C3})$$

where the basis $|j, k\rangle \in \mathcal{H}_j^k$ is the eigenstate of $J^2 = J_x^2 + J_y^2 + J_z^2$ and J_z , with $J_\alpha = \sum_i \sigma_i^\alpha$ for $\alpha = x, y, z$, i.e., $J^2|j, k\rangle = j(j+1)|j, k\rangle$ and $J_z|j, k\rangle = (k - N/2)|j, k\rangle$. From the above expression, this model satisfies the condition

$$\dim(\mathcal{H}_j^k) = 1. \quad (\text{C4})$$

We also note that $\dim(\mathcal{K}_j^k) = {}_N C_{N/2-j} - {}_N C_{N/2-j-1}$ and $\dim(\mathcal{S}_k) = \mathcal{N}_k = {}_N C_k = \sum_{j=|N/2-k|}^{N/2} \dim(\mathcal{K}_j^k)$. Moreover, $\dim(\mathcal{K}_{j_{\text{sym}}}^k) = 1$, and the basis

$$|\psi_k^{\text{sym}}\rangle = |j_{\text{sym}}, k\rangle = \frac{1}{\sqrt{{}_N C_k}} \sum_{g \in S_N} V_g^k |e\rangle^{\otimes k} \otimes |g\rangle^{\otimes N-k}, \quad (\text{C5})$$

is known as the symmetric Dicke states, satisfying $V_g|\psi_k^{\text{sym}}\rangle = V_g^k|\psi_k^{\text{sym}}\rangle = |\psi_k^{\text{sym}}\rangle$ for all $g \in S_N$. Therefore, $\rho_k^{\text{sym}} = |\psi_k^{\text{sym}}\rangle\langle\psi_k^{\text{sym}}|$ satisfies the condition (A22).

2. symmetric jump operator

The symmetric jump operator given in the main text reads

$$L_{\omega_0}^{\text{sym}} = \sum_{m=0}^{\lceil N/2 \rceil - 1} L_{\omega_0}^{(m)}, \quad (\text{C6})$$

and its approximation by taking the first $2n + 1$ -body terms reads

$$L_{\omega_0}^{2n+1\text{-ap}} = \sum_{m=0}^n L_{\omega_0}^{(m)}. \quad (\text{C7})$$

Here, the $L^{(m)}$ is defined as

$$L_{\omega_0}^{(m)} = \sum_{(i_1 < \dots < i_{m+1}) \neq (k_1 < \dots < k_m)} \sigma_{i_1}^- \cdots \sigma_{i_{m+1}}^- \sigma_{k_1}^+ \cdots \sigma_{k_m}^+. \quad (\text{C8})$$

To calculate the average jump rate, we use the following relation

$$L_{\omega_0}^{(m)} |\psi_k^{\text{sym}}\rangle = \sqrt{k(N-k+1)} [1 + f(N, k, m)] |\psi_{k-1}^{\text{sym}}\rangle, \quad (\text{C9})$$

where

$$f(N, k, m) = \frac{(N-k) \cdots (N-k+1-m)}{(m+1)!} \frac{(k-1) \cdots (k-m)}{m!}, \quad (\text{C10})$$

and $f(N, k, m=0) = 0$. The prefactor in front of Eq. (C9) can be understood as follows. If we fix $\sigma_{i_1}^-$, other σ^- 's acting on the Dicke state have the multiplicity $(k-1) \cdots (k-m)$, and σ^+ 's acting on the Dicke state have the multiplicity $(N-k) \cdots (N-k+1-m)$. Finally, the factor $k(N-k+1)$ arises from the Klein-Gordon coefficient for SU(2) operators: $J_- |\psi_k^{\text{sym}}\rangle = \sqrt{k(N-k+1)} |\psi_{k-1}^{\text{sym}}\rangle$, with $J_- = \sum_i \sigma_i^-$. Using Eq. (C9), we find that

$$A_{\omega_0}(\rho^{\text{sym}}, L_{\omega_0}^{2n+1\text{-ap}}) = c_k(L_{\omega_0}^{2n+1\text{-ap}}) \sum_{m=0}^n {}_{N-k+1}C_{m+1} \cdot {}_{k-1}C_{k-1-m}, \quad (\text{C11})$$

and

$$c_k(L_{\omega_0}^{2n+1\text{-ap}}) = \frac{k}{N-k+1} \sum_{m=0}^n {}_{N-k+1}C_{m+1} \cdot {}_{k-1}C_{k-1-m} \gamma_{\downarrow}. \quad (\text{C12})$$

Finally, we take $n = \lceil N/2 \rceil - 1$ and show the relation

$$A_{\omega_0}(\rho^{\text{sym}}, L_{\omega_0}^{\text{sym}}) = c_k(L_{\omega_0}^{\text{sym}})_N C_k, \quad (\text{C13})$$

and

$$c_k(L_{\omega_0}^{\text{sym}}) = \frac{k}{N-k+1} {}_N C_k \gamma_{\downarrow}. \quad (\text{C14})$$

If $k \geq \lceil N/2 \rceil$, we find that $\sum_{m=0}^{\lceil N/2 \rceil - 1} {}_{N-k+1}C_{m+1} \cdot {}_{k-1}C_{k-1-m} = \sum_{m=0}^{N-k} {}_{N-k+1}C_{N-k-m} \cdot {}_{k-1}C_m$. By using Vandermonde's identity $\sum_{m=0}^a {}_b C_m \cdot {}_c C_{a-m} = {}_{b+c} C_a$ for $a = N-k, b = k-1, c = N-k+1$, we obtain Eq. (C13). Next, we consider the case $k \leq \lceil N/2 \rceil$. In this case, we find that $\sum_{m=0}^{\lceil N/2 \rceil - 1} {}_{N-k+1}C_{m+1} \cdot {}_{k-1}C_{k-1-m} = \sum_{m=0}^{k-1} {}_{N-k+1}C_{m+1} \cdot {}_{k-1}C_{k-1-m} = \sum_{j=1}^k {}_{N-k+1}C_j \cdot {}_{k-1}C_{k-j}$, where the last equality is obtained by changing the variable to $j = m+1$. We then extend the summation to the case of $j = 0$, since ${}_{k-1}C_k = 0$. Finally, we use Vandermonde's identity and obtain Eq. (C13).

3. local jump operators

There are many choices for the local jump operators. In particular, for each

$$L_{a, \omega_0}^{2n+1\text{-ap}} = \sum_i \sigma_i^- + \sum_{(i_1 < i_2) \neq l_1} \sigma_{i_1}^- \sigma_{i_2}^- \sigma_{l_1}^+ + \cdots + \sum_{(i_1 < \dots < i_{n+1}) \neq (l_1 < \dots < l_n)} \sigma_{i_1}^- \cdots \sigma_{i_{n+1}}^- \sigma_{l_1}^+ \cdots \sigma_{l_n}^+, \quad (\text{C15})$$

we can construct a local jump operator with the same normalization factor c_k . The explicit form of the local jump operators that contain up to $2n+1$ -body jump operators read

$$\{L_{a,\omega_0}^{2n+1-\text{loc}}\} = \{\{\sigma_i^-\}, \{\sigma_{i_1}^-\sigma_{i_2}^-\sigma_{l_1}^+\}, \dots, \{\sigma_{i_1}^-\dots\sigma_{i_{n+1}}^-\sigma_{l_1}^+\dots\sigma_{l_n}^+\}\}. \quad (\text{C16})$$

Each element of Eq. (C16) satisfies the condition Eq. (A20). The master equation reads

$$\partial_t \rho = -i[H, \rho] + \gamma_{\downarrow} \left(\sum_i \mathcal{D}[\sigma_i] + \sum_{(i_1 < i_2) \neq l_1} \mathcal{D}[\sigma_{i_1}^-\sigma_{i_2}^-\sigma_{l_1}^+] + \dots + \sum_{(i_1 < \dots < i_{n+1}) \neq (l_1 < \dots < l_n)} \mathcal{D}[\sigma_{i_1}^-\dots\sigma_{i_{n+1}}^-\sigma_{l_1}^+\dots\sigma_{l_n}^+] \right) \rho, \quad (\text{C17})$$

where $\mathcal{D}[L]\rho = L\rho L^\dagger - (1/2)\{L^\dagger L, \rho\}$ is the dissipator. Note that Eq. (C17) satisfies the weak symmetry [1]. An argument similar to that below Eq. (C10) leads to

$$A_{\omega_0}(\rho, \{L_{a,\omega_0}^{2n+1-\text{loc}}\}) = \sum_k p_k c_k(\{L_{a,\omega_0}^{2n+1-\text{loc}}\}), \quad (\text{C18})$$

and $c_k(\{L_{a,\omega_0}^{2n+1-\text{loc}}\}) = c_k(L_{\omega_0}^{2n+1-\text{ap}})$. Note that the jump operators act individually on the system in the case of $\{L_{a,\omega_0}^{2n+1-\text{loc}}\}$, whereas they act collectively in the case of $L_{\omega_0}^{2n+1-\text{ap}}$. They share same number of operators involved in their expression, and thus the Hilbert-Schmidt norm of the jump operators $c_k(\{L_{a,\omega_0}^{2n+1-\text{loc}}\})$ and $c_k(L_{\omega_0}^{2n+1-\text{ap}})$ take the same value.

4. Scaling of A

We now discuss the scaling behavior of A . Let us first assume that the explicit form of the master equation reads

$$\partial_t \rho = -i[H, \rho] + \gamma_{\downarrow} \mathcal{D}[L_{\omega_0}] \rho + \gamma_{\uparrow} \mathcal{D}[L_{\omega_0}^\dagger] \rho, \quad (\text{C19})$$

with $L_{\omega_0} = \{L_{\omega_0}^{1-\text{ap}}, L_{\omega_0}^{3-\text{ap}}, L_{\omega_0}^{\text{sym}}\}$, $\gamma_{\downarrow} = \Gamma_0/(1 + e^{-\beta\omega_0})$ and $\gamma_{\uparrow} = \Gamma_0/(1 + e^{\beta\omega_0})$ satisfy the detailed balance condition $\gamma_{\downarrow}/\gamma_{\uparrow} = e^{\beta\omega_0}$. These jump operators satisfy the strong symmetry condition, and therefore the steady-state depends on the initial state. If the initial state is prepared in the so-called symmetric Dicke subspace (e.g., $\rho(0) = \sum_{k,j} \rho_{k,j} |\psi_k^{\text{sym}}\rangle\langle\psi_j^{\text{sym}}|$), the steady-state is given by the thermal state within this subspace:

$$\rho_{\text{th}}^{\text{sym}} = \sum_k p_k^{\text{th}} |\psi_k^{\text{sym}}\rangle\langle\psi_k^{\text{sym}}|, \quad (\text{C20})$$

where $p_k^{\text{th}} = e^{-k\beta\omega}/Z$ and $Z = \sum_{k=0}^N e^{-k\beta\omega}$.

The explicit form of $A = \sum_{\omega=\pm\omega_0} \omega^2 A_{\omega}(\rho^{\text{sym}}, L_{\omega})$, with $\rho^{\text{sym}} = \sum_k p_k |\psi_k^{\text{sym}}\rangle\langle\psi_k^{\text{sym}}|$ is given by

$$A^{1-\text{ap}} = \omega_0^2 \sum_k p_k [\gamma_{\downarrow} k(N-k+1) + \gamma_{\uparrow} (k+1)(N-k)], \quad (\text{C21})$$

$$A^{3-\text{ap}} = \omega_0^2 \sum_k p_k \left(\gamma_{\downarrow} k(N-k+1)[1 + (k-1)(N-k)/2]^2 + \gamma_{\uparrow} (k+1)(N-k)[1 + k(N-k-1)/2]^2 \right), \quad (\text{C22})$$

$$A^{\text{sym}} = \omega_0^2 \sum_k p_k \left[\gamma_{\downarrow} ({}_N C_k)^2 \frac{k}{N-k+1} + \gamma_{\uparrow} ({}_N C_{k+1})^2 \frac{k+1}{N-k} \right]. \quad (\text{C23})$$

In Fig. 5, we plot Eqs. (C21), (C22), and (C23) when the density matrix of the system is given by $\rho_{\text{th}}^{\text{sym}}$ [Eq. (C20)]. Note that for large N , the scaling behavior $A^{1-\text{ap}} = O(N)$ and $A^{3-\text{ap}} = O(N^3)$ can be analytically obtained as well by noting that $\sum_k p_k^{\text{th}} k^n = O(1)$ for $n = 0, 1, \dots$. The red curve shows that A^{sym} scales exponentially.

Next, we assume that the jump operators are given by $\{\sigma_i^-\}$ and $\{\sigma_i^+\}$. The master equation reads

$$\partial_t \rho = -i[H, \rho] + \gamma_{\downarrow} \sum_{i=1}^N \mathcal{D}[\sigma_i^-] \rho + \gamma_{\uparrow} \sum_{i=1}^N \mathcal{D}[\sigma_i^+] \rho. \quad (\text{C24})$$

In this case, the jump operator does not satisfy the strong symmetry condition, and the steady-state of Eq. (C24) is

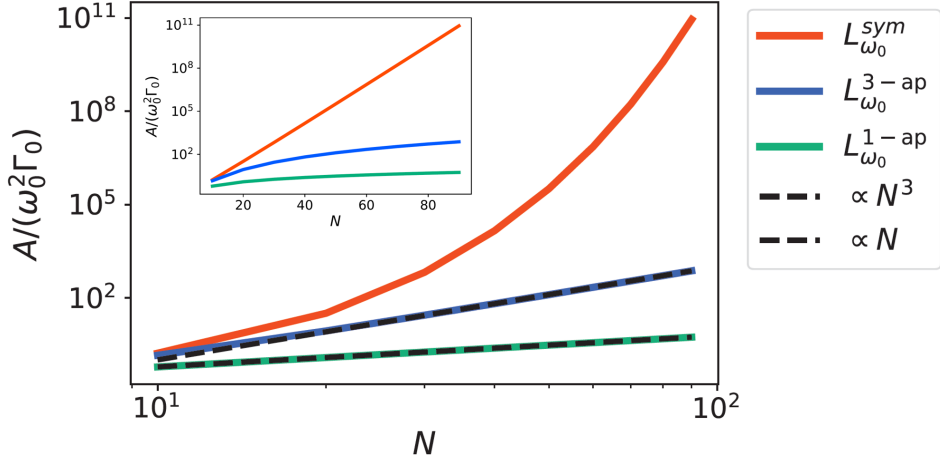


FIG. 5. Scaling of A for different jump operators when the density matrix is given by $\rho_{\text{th}}^{\text{sym}}$ (C20). The figure shows that A scales $O(N)$ for $L_{\pm\omega_0}^{1\text{-ap}}$ and $O(N^3)$ for $L_{\pm\omega_0}^{3\text{-ap}}$. We use a semi-log plot in the inset, which shows an exponential scaling of A for the symmetric jump operator $L_{\pm\omega_0}^{\text{sym}}$. The parameters are $\omega_0 = 0.7$, $\beta = 5$.

uniquely given by a thermal state

$$\rho_{\text{th}} = \frac{e^{-\beta H}}{\text{Tr}[e^{-\beta H}]} = \sum_k p_k^{\text{th}} \Pi_k. \quad (\text{C25})$$

Because Eq. (C25) satisfies the condition (A20), we find that $A_{\omega}(\rho_{\text{th}}, \{L_{a,\omega}\}) = \sum_k p_k^{\text{th}} c_k(L_{a,\omega})$ for any jump operators. The explicit form of A using jump operators $\{\sigma_i^-\}$ and $\{\sigma_i^+\}$ reads

$$A^{\text{loc}} = \omega_0^2 \sum_k p_k [\gamma_{\downarrow} k + \gamma_{\uparrow} (N - k)]. \quad (\text{C26})$$

Appendix D: Details on the quantum heat engine model

In this section we provide details on the quantum heat engine model discussed in the main text. The time evolution of the system reads

$$\partial_t \rho = \mathcal{L}_j \rho = -i[H_j, \rho] + \sum_{a,\omega} \gamma_{a,\omega}^j \mathcal{D}[L_{a,\omega}] \rho, \quad (\text{D1})$$

where $j = \{H, C\}$ labels whether the system is interacting with the hot bath (H) or the cold bath (C), and $H_j = (\omega_j/2) \sum_{i=1}^N \sigma_i^z$ is the Hamiltonian of the system. We assume the detailed balance condition $\gamma_{a,\omega}^j = e^{\beta_j \omega_j} \gamma_{a,-\omega}^j$, where β_j is the inverse temperature of the heat bath.

We consider a standard quantum Otto cycle, where the four-stroke protocol reads

1. Investing work via changing the frequency of the system $\omega_C \rightarrow \omega_H$.
2. Absorbing heat $Q_H \geq 0$ with the hot bath at inverse temperature β_H for a time-duration τ_H , using Eq. (D1).
3. Extracting work via changing the frequency of the system $\omega_H \rightarrow \omega_C$.
4. Releasing heat $Q_C \geq 0$ to the cold bath at inverse temperature β_C for a time-duration τ_C , using Eq. (D1).

Using the first law of thermodynamics, the extracted work reads $W = Q_H - Q_C$. The performance of the heat engine is quantified by the heat-to-work conversion efficiency $\eta = W/Q_H$, and the output power $P = W/(\tau_H + \tau_C)$. In steps 1 and 3, we assume that the system is detached from the heat bath. Suppose that we write the time-dependence of the Hamiltonian during step 1 as $H(t) = (\omega(t)/2) \sum_{i=1}^N \sigma_i^z$, where $\omega(t)$ denotes the time-dependence of changing

the frequency of the Hamiltonian from $\omega(t_{\text{ini}}) = \omega_C$ to $\omega(t_{\text{fin}}) = \omega_H$. We note that the Hamiltonian of the system during step 1 (and also step 3) commutes with each other at different times, i.e., $[H(t), H(t')] = 0$. In particular, the occupation probabilities p_k 's of the energy eigenstates are unchanged during steps 1 and 3, regardless of the speed of changing $\omega(t)$. Therefore, typical detrimental effects on the power and efficiency of heat engines that occur for fast and non-commuting Hamiltonian protocols ($[H(t), H(t')] \neq 0$) do not occur in the above protocol. From the above consideration, we assume that steps 1 and 3 can be completed instantaneously, and identify the total cycle time as $\tau_H + \tau_C$. See also the analysis of a sudden cycle [50] which corresponds to a heat engine protocol with steps 1 and 3 done instantaneously for both commuting and non-commuting Hamiltonians. The above protocol realizes a heat engine cycle when $\beta_H \omega_H \geq \beta_C \omega_C$.

When the engine cycle becomes stationary, the density matrix at the beginning of step 1 satisfies the condition $\rho_1 = e^{\mathcal{L}_C \tau_C} e^{\mathcal{L}_H \tau_H} \rho_1$. The work and heat read

$$W = (\omega_H - \omega_C) \sum_{i=1}^N \text{Tr}[\sigma_i^z (e^{\mathcal{L}_H \tau_H} - 1) \rho_1]. \quad (\text{D2})$$

Similarly, the heat reads

$$Q_H = \omega_H \sum_{i=1}^N \text{Tr}[\sigma_i^z (e^{\mathcal{L}_H \tau_H} - 1) \rho_1] \quad (\text{D3})$$

$$Q_C = -\omega_C \sum_{i=1}^N \text{Tr}[\sigma_i^z (e^{\mathcal{L}_C \tau_C} e^{\mathcal{L}_H \tau_H} - e^{\mathcal{L}_H \tau_H}) \rho_1]. \quad (\text{D4})$$

From Eqs. (D2) and (D3), the efficiency reads

$$\eta = \frac{W}{Q_H} = 1 - \frac{\omega_C}{\omega_H}, \quad (\text{D5})$$

which is identical to the Otto efficiency. By choosing

$$\omega_C = \frac{\beta_H}{\beta_C} \omega_H + \frac{b}{N} \omega_H, \quad (\text{D6})$$

the difference between the Carnot efficiency $\eta_{\text{Car}} = 1 - \beta_H / \beta_C$ and the efficiency reads

$$\eta_{\text{Car}} - \eta = \frac{b}{N} = O(1/N). \quad (\text{D7})$$

In the numerical simulation, we fix $b = 0.1, \omega_H = 0.7, \beta_H = 5, \beta_C = 8$ and use Eq. (D6) to determine ω_C . We also consider the form $\gamma_{a,\omega_j}^j = \gamma_{\downarrow}^j = \Gamma_0 / (1 + e^{-\beta_j \omega_j})$ and $\gamma_{a,-\omega_j}^j = \gamma_{\uparrow}^j = \Gamma_0 / (1 + e^{\beta_j \omega_j})$, and set $\Gamma_0 = 0.2$ in the numerical simulation. We numerically optimize the output power for $N = 1$ by varying τ_H and τ_C , and find that $\tau_H^{N=1} = 0.168, \tau_C^{N=1} = 0.180$. For $N > 2$, we choose $\tau_H = \tau_H^{N=1} N^{-3}$ and $\tau_C = \tau_C^{N=1} N^{-3}$ for $L_{\omega_0}^{\text{1-ap}}$ and $L_{\omega_0}^{\text{3-ap}}$. We also choose $\tau_H = \tau_H^{N=1} N^{-6}$ and $\tau_C = \tau_C^{N=1} N^{-6}$ for $L_{\omega_0}^{\text{sym}}$. Using these parameters, we obtain the numerical plot in the main text by considering three different jump operators $L_{\omega_0}^{\text{1-ap}}, L_{\omega_0}^{\text{3-ap}}$, and $L_{\omega_0}^{\text{sym}}$. Here, we assume that the initial state is prepared by the symmetric Dicke state. Then, the time-evolution of the system is confined in the subspace spanned by the symmetric Dicke states by noting that all jump operators satisfy the strong symmetry condition [1]. In Fig. 7, we show additional plots of the output power by using the local jump operators.

The explicit form of the master equation reads

$$\partial_t \rho = -i[H_j, \rho] + \gamma_{\downarrow}^j \mathcal{D}[L_{\omega_0}] \rho + \gamma_{\uparrow}^j \mathcal{D}[L_{\omega_0}^{\dagger}] \rho, \quad (\text{D8})$$

with $L_{\omega_0} = \{L_{\omega_0}^{\text{1-ap}}, L_{\omega_0}^{\text{3-ap}}, L_{\omega_0}^{\text{sym}}\}$.

The analytical expression of \bar{A} using $L_{\omega_0}^{\text{1-ap}}$ reads

$$\bar{A}^{\text{1-ap}} = \omega_0^2 \sum_k [\bar{p}_k \gamma_{\downarrow}^j k(N - k + 1) + \bar{p}_k \gamma_{\uparrow}^j (k + 1)(N - k)] \quad (\text{D9})$$

where $\bar{p}_k \gamma_{\downarrow}^j = (\int_0^{\tau_H} dt p_k(t) \gamma_{\downarrow}^H + \int_{\tau_H}^{\tau_C + \tau_H} dt p_k(t) \gamma_{\downarrow}^H) / (\tau_H + \tau_C)$ denotes the short-hand notation of the time-average

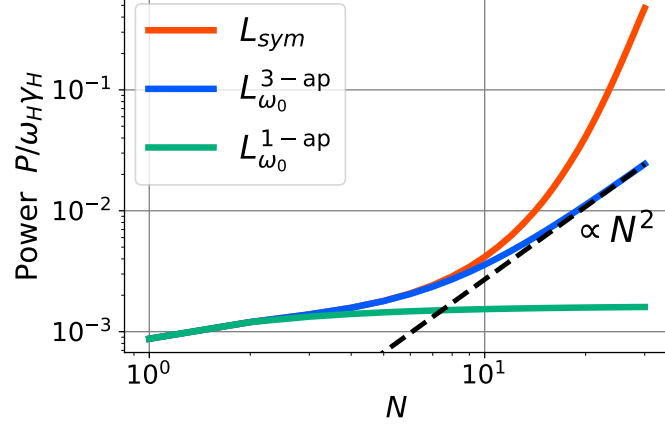


FIG. 6. Plot of the power of the permutation invariant N two-level system heat engine using the log-log plot. Here, the black dashed line is added to show the N^2 scaling of the power when we use $L_{\omega_0}^{3\text{-ap}}$.

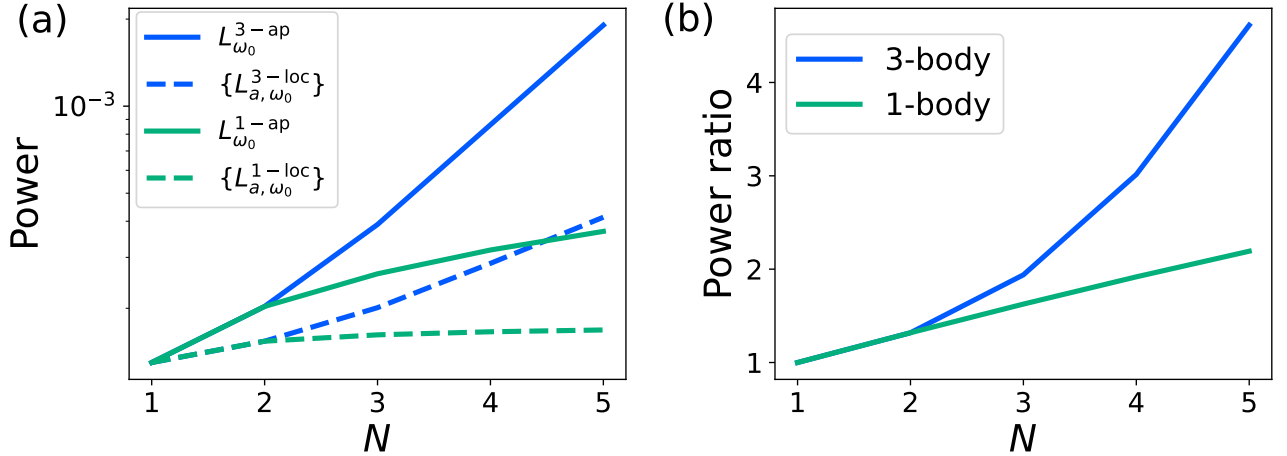


FIG. 7. (a) Plot of the output power of heat engines for different jump operators $L_{\omega_0}^{3\text{-ap}}$, $\{L_{a,\omega_0}^{3\text{-loc}}\}$, $L_{\omega_0}^{1\text{-ap}}$, $\{L_{a,\omega_0}^{1\text{-loc}}\}$. (b) Plot of the ratio of the power between jump operators $L_{\omega_0}^{2n+1\text{-ap}}$ and $\{L_{a,\omega_0}^{2n+1\text{-loc}}\}$ for 1-body ($n = 0$) and 3-body ($n = 1$) terms. The blue curve is given by $P^{3\text{-ap}}/P^{3\text{-loc}}$ and the green curve is given by $P^{1\text{-ap}}/P^{1\text{-loc}}$. The parameters are $b = 0.1$, $\omega_H = 0.7$, $\beta_H = 0.5$, $\beta_C = 0.8$, $\Gamma_0 = 0.2$.

over one cycle. Similar relation holds for $\bar{p}_k\bar{\gamma}_{\uparrow}$ as well. Here, we assume that the population of k -th symmetric Dicke state $|\psi_k^{\text{sym}}\rangle$ follows an exponential form $\ln p_k \propto -k$. In this case, we find

$$\bar{A}^{1\text{-ap}} = O(N). \quad (\text{D10})$$

Similarly, the analytical expression of \bar{A} using $L_{\omega_0}^{3\text{-ap}}$ reads

$$\bar{A}^{3\text{-ap}} = \omega_0^2 \sum_k (\bar{p}_k \bar{\gamma}_{\downarrow} k (N - k + 1) [1 + (k - 1)(N - k)/2]^2 + \bar{p}_k \bar{\gamma}_{\uparrow} (k + 1)(N - k) [1 + k(N - k - 1)/2]^2). \quad (\text{D11})$$

By assuming the form $\ln p_k \propto -k$, we find

$$\bar{A}^{3\text{-ap}} = O(N^3). \quad (\text{D12})$$

Let us now recall the power-efficiency trade-off relation [20, 33] [Eq. (11) in the main text]:

$$\frac{P}{\eta_{\text{Car}} - \eta} \leq c\bar{A}, \quad (\text{D13})$$

where $\eta_{\text{Car}} = 1 - \beta_H/\beta_C$ is the Carnot efficiency; β_H and β_C are the inverse temperatures of the hot and cold baths; $c = \beta_C \eta_{\text{Car}} / [2(2 - \eta_{\text{Car}})^2]$ is a constant; and $\bar{A} = \tau^{-1} \int_0^\tau dt \sum_{\omega,k} \omega^2 p_k c_k \mathcal{A}_\omega(\rho_k, \{L_{a,\omega}\})$, where τ is the duration of time to complete one engine cycle. In Ref. [20], the authors discussed that if \bar{A} scales as $O(\mathcal{N}^2)$, where \mathcal{N} is the number of degeneracy, then the scaling $P = O(\mathcal{N})$ and $\eta_{\text{Car}} - \eta = O(1/\mathcal{N})$ becomes possible. Moreover, an explicit model that realizes such scaling behavior has been introduced (see also Sec. E). Similarly, if \bar{A} scales as $O(\mathcal{N}^{\alpha+1})$ and the efficiency scales as $\eta_{\text{Car}} - \eta = O(1/\mathcal{N})$ as in Eq. (D7), the power scales as $P = O(\mathcal{N}^\alpha)$ when the inequality in Eq. (D13) is saturated. Therefore, realizing a model with $\alpha \geq 1$ is practically important, because such scaling allows obtaining the power which is nonvanishing in the macroscopic limit ($N \rightarrow \infty$) while approximately attaining the Carnot efficiency [20]. Indeed, Fig. 6 shows that for large N , the power scales as

$$P^{\text{3-ap}} = O(N^2) \quad (\text{D14})$$

while the efficiency scales as

$$\eta_{\text{Car}} - \eta = O(1/\mathcal{N}). \quad (\text{D15})$$

To realize this $O(N^2)$ enhancement via $L_{\pm\omega_0}^{\text{3-ap}}$, the system-bath interaction Hamiltonian requires the form $H_{\text{int}} = S \otimes B$, where B is the bath operator and $S = \sum_i \sigma_i^x + \sum_{i < j < k} \sigma_i^x \otimes \sigma_j^x \otimes \sigma_k^x$ is the system operator. An interesting future direction is to find a setup that realizes this non-linear system-bath coupling, for example, using the nonlinear interactions [52], or the digital simulations of open quantum systems via trapped ion platforms [53–56].

Appendix E: Details on the permutation and even number bit flip invariance example

In this section, we give further details on the permutation and even number bit flip invariant system discussed in the main text. The Hamiltonian reads

$$H = \epsilon \prod_{i=1}^N \sigma_i^z. \quad (\text{E1})$$

The Hamiltonian (E1) has two eigen-energies $\pm\epsilon$, and the number of degeneracies are $\mathcal{N}_{\pm\epsilon} = \mathcal{N} = 2^{N-1}$. The projection operators to the energy eigenspace read $\Pi_{\pm\epsilon} = \frac{1}{2}(1 \pm \prod_i \sigma_i^z)$. The Hamiltonian (E1) is permutation invariant, and it is also invariant under an even number bit flip operation

$$\{U_g\} = \{1, \sigma_{i_1}^x \sigma_{i_2}^x, \sigma_{i_1}^x \sigma_{i_2}^x \sigma_{i_3}^x \sigma_{i_4}^x, \dots\}. \quad (\text{E2})$$

An explicit calculation reads $[H, U_g] = [\Pi_{\pm\epsilon}, U_g] = 0$.

1. Permutation symmetry and block diagonal structure

In this subsection, we first consider only the permutation group S_N and consider decomposing the energy eigenspace $\mathcal{S}_{\pm\epsilon}$. Using the irreducible representations of S_N , we have the block diagonal structure

$$\mathcal{S}_k = \bigoplus_{j=j_{\text{min}}}^{j_{\text{sym}}} \mathcal{H}_j^k \otimes \mathcal{K}_j^k, \quad (\text{E3})$$

where j labels the irreducible representations of S_N , $k = \pm\epsilon$, $j_{\text{sym}} = N/2$, and $j_{\text{min}} = 1/2$ if N is odd and $j_{\text{min}} = 0$ if N is even. The projection operator $\Pi_{\pm\epsilon}$ can be decomposed as

$$\Pi_{\pm\epsilon} = \bigoplus_{j=j_{\text{min}}}^{j_{\text{sym}}} \sum_m |j, m\rangle \langle j, m| \otimes I_{\mathcal{K}_j^{\pm\epsilon}}. \quad (\text{E4})$$

If N is even (odd), the summation over m is taken only for even (odd) numbers within the range $m = j - N/2, \dots, j + N/2$. We note that $\Pi_{-\epsilon}$ can be decomposed into a similar form. What should be noted here is that

$$\dim(\mathcal{H}_j^k) \neq 1, \quad (\text{E5})$$

and for example, $\dim(\mathcal{H}_{j_{\text{sym}}}^{+\epsilon}) = \lceil (N+1)/2 \rceil$. However, the subspace \mathcal{H}_j^k is not invariant under the even number bit-flip operation, and thus it can be further decomposed.

2. Local and symmetric states

The local energy eigenbasis for $\mathcal{S}_{\pm\epsilon}$ are given by ($V'_g = V_{g_1}U_{g_2}$ with $g = (g_1, g_2)$)

$$\begin{aligned} \mathcal{B}_{+\epsilon}^{\text{loc}} &= \{|\psi_{+\epsilon}^{\text{loc}}(\alpha)\rangle\} = \{V'_g|e\rangle^{\otimes N}\}_{g \in G}, \\ \mathcal{B}_{-\epsilon}^{\text{loc}} &= \{|\psi_{-\epsilon}^{\text{loc}}(\alpha)\rangle\} = \{V'_g|g\rangle \otimes |e\rangle^{\otimes N-1}\}_{g \in G}. \end{aligned} \quad (\text{E6})$$

In particular, we find that

$$\frac{1}{|G|} \sum_g V_g |\psi_{\pm\epsilon}^{\text{loc}}(\alpha)\rangle \langle \psi_{\pm\epsilon}^{\text{loc}}(\alpha)| V_g^\dagger = \frac{1}{\mathcal{N}} \Pi_{\pm\epsilon}, \quad (\text{E7})$$

and there is no nontrivial subspace in $\mathcal{S}_{\pm\epsilon}$ under the action of V'_g , meaning that $\dim(\mathcal{H}_j^k) = 1$ by considering V'_g .

In addition, the symmetric state is uniquely given by $\rho_{\pm\epsilon}^{\text{sym}} = |\psi_{\pm\epsilon}^{\text{sym}}\rangle\langle\psi_{\pm\epsilon}^{\text{sym}}|$, with

$$|\psi_{\pm\epsilon}^{\text{sym}}\rangle = \frac{1}{\sqrt{2}} (|+\rangle^{\otimes N} \pm |-\rangle^{\otimes N}), \quad (\text{E8})$$

where $|\pm\rangle = (|e\rangle \pm |g\rangle)/\sqrt{2}$. One can check that it is invariant under the permutation $\{V_g\}_{g \in S_N}$ and Eq. (E2). By taking the superposition of local states (E6), we obtain that

$$|\psi_{\pm\epsilon}^{\text{sym}}\rangle = \frac{1}{\sqrt{\mathcal{N}}} \sum_{g \in G} V'_g |\psi_{\pm\epsilon}^{\text{loc}}\rangle. \quad (\text{E9})$$

3. Local and symmetric jump operators

The symmetric jump operator is given by

$$\begin{aligned} L_{2\epsilon}^{\text{sym}} &= \sum_{m=0}^{\lceil N/2 \rceil - 1} \sum_{i_1 < \dots < i_{2m+1}} \Pi_{-\epsilon} \sigma_{i_1}^x \cdots \sigma_{i_{2m+1}}^x \Pi_{\epsilon} \\ &= \Pi_{-\epsilon} \prod_i (\sigma_i^x + 1) \Pi_{\epsilon} \\ &= \mathcal{N} |\psi_{-\epsilon}^{\text{sym}}\rangle\langle\psi_{\epsilon}^{\text{sym}}|, \end{aligned} \quad (\text{E10})$$

with

$$\mathcal{A}_{2\epsilon}(\rho_{\epsilon}^{\text{sym}}, L_{2\epsilon}^{\text{sym}}) = \mathcal{N} c_{\epsilon}^{\text{sym}} \quad (\text{E11})$$

and $c_{\epsilon}^{\text{sym}} = \gamma_{\downarrow} \mathcal{N}$.

We can similarly take the first $2n+1$ -body term approximation and find

$$L_{2\epsilon}^{2n+1-\text{ap}} = \sum_{m=0}^n \sum_{i_1 < \dots < i_{2m+1}} \Pi_{-\epsilon} \sigma_{i_1}^x \cdots \sigma_{i_{2m+1}}^x \Pi_{\epsilon}, \quad (\text{E12})$$

with

$$A_{2\epsilon}(\rho_{\epsilon}^{\text{sym}}, L_{2\epsilon}^{2n+1-\text{ap}}) = \sum_{m=0}^n {}_N C_{2m+1} c_k^{2n+1-\text{ap}} \quad (\text{E13})$$

and $c_k^{2n+1-\text{ap}} = \gamma_{\downarrow} \sum_{m=0}^n {}_N C_{2m+1}$.

Now, local jump operators can be obtained

$$\{L_{a,2\epsilon}^{2n+1-\text{loc}}\} = \left\{ \{\Pi_{-\epsilon} \sigma_{i_1}^x \Pi_{\epsilon}\}, \{\Pi_{-\epsilon} \sigma_{i_1}^x \sigma_{i_2}^x \sigma_{i_3}^x \Pi_{\epsilon}\}, \dots, \{\Pi_{-\epsilon} \sigma_{i_1}^x \dots \sigma_{i_{2m+1}}^x \Pi_{\epsilon}\} \right\}. \quad (\text{E14})$$

These jump operators satisfy $A_{2\epsilon}(\rho_{\epsilon}^{\text{sym}}, L_{a,2\epsilon}^{2n+1-\text{loc}}) = c_k^{2n+1-\text{loc}}$ and $c_k^{2n+1-\text{loc}} = c_k^{2n+1-\text{ap}}$.

Note that this permutation and even number bit flip invariant model corresponds to the $2\mathcal{N}$ -state model discussed in Ref. [20] by noting that $A = O(\mathcal{N}^2)$. Therefore, by applying the results discussed in Ref. [20], we can realize a heat engine model that achieves $\eta_{\text{Car}} - \eta = O(1/\mathcal{N})$ and $P = O(\mathcal{N})$.

In Ref. [51], the authors impose a condition on the size of the system coupling operator $\|S_a\|$ and derive a bound on the heat current. On the other hand, our enhancement analysis is based on comparing different states and jump operators by excluding the difference of the normalization factor c_k . Note that we can renormalize the coefficient of the jump operators and set c_k to be the same value in the above example as well.

[1] B. Buča and T. Prosen, A note on symmetry reductions of the lindblad equation: transport in constrained open spin chains, *New Journal of Physics* **14**, 073007 (2012).

[2] V. V. Albert and L. Jiang, Symmetries and conserved quantities in lindblad master equations, *Phys. Rev. A* **89**, 022118 (2014).

[3] K. Kawabata, K. Shiozaki, M. Ueda, and M. Sato, Symmetry and topology in non-hermitian physics, *Phys. Rev. X* **9**, 041015 (2019).

[4] E. J. Bergholtz, J. C. Budich, and F. K. Kunst, Exceptional topology of non-hermitian systems, *Rev. Mod. Phys.* **93**, 015005 (2021).

[5] C.-E. Bardyn, M. A. Baranov, C. V. Kraus, E. Rico, A. İmamoğlu, P. Zoller, and S. Diehl, Topology by dissipation, *New Journal of Physics* **15**, 085001 (2013).

[6] K. Kawabata, A. Kulkarni, J. Li, T. Numasawa, and S. Ryu, Symmetry of open quantum systems: Classification of dissipative quantum chaos, *PRX Quantum* **4**, 030328 (2023).

[7] R. El-Ganainy, K. G. Makris, M. Khajavikhan, Z. H. Musslimani, S. Rotter, and D. N. Christodoulides, Non-hermitian physics and pt symmetry, *Nature Physics* **14**, 11 (2018).

[8] C. M. Bender, Making sense of non-hermitian hamiltonians, *Reports on Progress in Physics* **70**, 947 (2007).

[9] G. Lindblad, On the generators of quantum dynamical semigroups, *Commun. Math. Phys.* **48**, 119 (1976).

[10] A. K. V. Gorini and E. C. G. Sudarshan, Completely positive dynamical semigroups of N-level systems, *Journal of Mathematical Physics* **17**, 821 (2008).

[11] H.-P. Breuer and F. Petruccione, *The Theory of Open Quantum Systems* (Oxford University Press, 2002).

[12] Z. Nussinov and G. Ortiz, A symmetry principle for topological quantum order, *Annals of Physics* **324**, 977 (2009).

[13] D. A. Lidar, Review of decoherence-free subspaces, noiseless subsystems, and dynamical decoupling, in *Quantum Information and Computation for Chemistry* (John Wiley & Sons, Ltd, 2014) pp. 295–354.

[14] R. H. Dicke, Coherence in spontaneous radiation processes, *Phys. Rev.* **93**, 99 (1954).

[15] B. M. Garraway, The dicke model in quantum optics: Dicke model revisited, *Philosophical Transactions of the Royal Society A: Mathematical, Physical and Engineering Sciences* **369**, 1137 (2011).

[16] D. Gelbwaser-Klimovsky, W. Niedenzu, P. Brumer, and G. Kurizki, Power enhancement of heat engines via correlated thermalization in a three-level “working fluid”, *Scientific reports* **5**, 14413 (2015).

[17] A. Ü. Hardal and Ö. E. Müstecaplıoğlu, Superradiant quantum heat engine, *Scientific reports* **5**, 12953 (2015).

[18] W. Niedenzu and G. Kurizki, Cooperative many-body enhancement of quantum thermal machine power, *New Journal of Physics* **20**, 113038 (2018).

[19] G. Watanabe, B. P. Venkatesh, P. Talkner, M.-J. Hwang, and A. del Campo, Quantum statistical enhancement of the collective performance of multiple bosonic engines, *Phys. Rev. Lett.* **124**, 210603 (2020).

[20] H. Tajima and K. Funo, Superconducting-like heat current: Effective cancellation of current-dissipation trade-off by quantum coherence, *Phys. Rev. Lett.* **127**, 190604 (2021).

[21] S. Kamimura, H. Hakoshima, Y. Matsuzaki, K. Yoshida, and Y. Tokura, Quantum-enhanced heat engine based on super-absorption, *Phys. Rev. Lett.* **128**, 180602 (2022).

[22] B. Yadin, B. Morris, and K. Brandner, Thermodynamics of permutation-invariant quantum many-body systems: A group-theoretical framework, *Phys. Rev. Res.* **5**, 033018 (2023).

[23] J. Kim, S.-h. Oh, D. Yang, J. Kim, M. Lee, and K. An, A photonic quantum engine driven by superradiance, *Nature Photonics* **16**, 707 (2022).

[24] F. C. Binder, S. Vinjanampathy, K. Modi, and J. Goold, Quantacell: powerful charging of quantum batteries, *New Journal of Physics* **17**, 075015 (2015).

[25] F. Campaioli, F. A. Pollock, F. C. Binder, L. Céleri, J. Goold, S. Vinjanampathy, and K. Modi, Enhancing the charging power of quantum batteries, *Phys. Rev. Lett.* **118**, 150601 (2017).

[26] J.-Y. Gyhm, D. Šafránek, and D. Rosa, Quantum charging advantage cannot be extensive without global operations, *Phys. Rev. Lett.* **128**, 140501 (2022).

[27] A. Rolandi, P. Abiuso, and M. Perarnau-Llobet, Collective advantages in finite-time thermodynamics, *Phys. Rev. Lett.* **131**, 210401 (2023).

[28] Y. Liu, C. Huang, X. Zhang, and D. He, Collective advantages in qubit reset: effect of coherent qubits, (2024), arXiv:2407.03096 [quant-ph].

[29] C. Creatore, M. A. Parker, S. Emmott, and A. W. Chin, Efficient biologically inspired photocell enhanced by delocalized quantum states, *Phys. Rev. Lett.* **111**, 253601 (2013).

[30] K. Funo, N. Shiraishi, and K. Saito, Speed limit for open quantum systems, *New Journal of Physics* **21**, 013006 (2019).

[31] T. Van Vu and K. Saito, Thermodynamic unification of optimal transport: Thermodynamic uncertainty relation, minimum dissipation, and thermodynamic speed limits, *Phys. Rev. X* **13**, 011013 (2023).

[32] T. Van Vu and Y. Hasegawa, Geometrical bounds of the irreversibility in markovian systems, *Phys. Rev. Lett.* **126**, 010601 (2021).

[33] N. Shiraishi and K. Saito, Fundamental relation between entropy production and heat current, *J Stat Phys* **174**, 433–468 (2019).

[34] S. Deffner and M. V. S. Bonança, Thermodynamic control —an old paradigm with new applications, *Europhysics Letters* **131**, 20001 (2020).

[35] P. Abiuso and M. Perarnau-Llobet, Optimal cycles for low-dissipation heat engines, *Phys. Rev. Lett.* **124**, 110606 (2020).

[36] M. Esposito, R. Kawai, K. Lindenberg, and C. Van den Broeck, Efficiency at maximum power of low-dissipation carnot engines, *Phys. Rev. Lett.* **105**, 150603 (2010).

[37] E. Aurell, C. Mejía-Monasterio, and P. Muratore-Ginanneschi, Optimal protocols and optimal transport in stochastic thermodynamics, *Phys. Rev. Lett.* **106**, 250601 (2011).

[38] R. Kosloff and Y. Rezek, The quantum harmonic otto cycle, *Entropy* **19**, 136 (2017).

[39] N. Shiraishi, K. Funo, and K. Saito, Speed limit for classical stochastic processes, *Phys. Rev. Lett.* **121**, 070601 (2018).

[40] N. Shiraishi, K. Saito, and H. Tasaki, Universal trade-off relation between power and efficiency for heat engines, *Phys. Rev. Lett.* **117**, 190601 (2016).

[41] In the supplemental material, we show general properties of A_ω for different states and jump operators, including its upper bound. We also give additional details on the setup, examples, and the heat engine setup shown in the main text. The supplemental material includes Ref. [50–56].

[42] A. Kitaev, Fault-tolerant quantum computation by anyons, *Annals of Physics* **303**, 2 (2003).

[43] R. Alicki, M. Šindelka, and D. Gelbwaser-Klimovsky, Violation of detailed balance in quantum open systems, *Phys. Rev. Lett.* **131**, 040401 (2023).

[44] H.-P. Breuer, E.-M. Laine, J. Piilo, and B. Vacchini, Colloquium: Non-markovian dynamics in open quantum systems, *Rev. Mod. Phys.* **88**, 021002 (2016).

[45] I. de Vega and D. Alonso, Dynamics of non-markovian open quantum systems, *Rev. Mod. Phys.* **89**, 015001 (2017).

[46] A. Metelmann and A. A. Clerk, Nonreciprocal photon transmission and amplification via reservoir engineering, *Phys. Rev. X* **5**, 021025 (2015).

[47] A. A. Clerk, Introduction to quantum non-reciprocal interactions: from non-Hermitian Hamiltonians to quantum master equations and quantum feedforward schemes, *SciPost Phys. Lect. Notes* , 44 (2022).

[48] R. Goodman, N. R. Wallach, *et al.*, *Symmetry, representations, and invariants*, Vol. 255 (Springer, 2009).

[49] P. Etingof, O. Golberg, S. Hensel, T. Liu, A. Schwendner, D. Vaintrob, and E. Yudovina, Introduction to representation theory, (2011), arXiv:0901.0827 [math.RT].

[50] J. P. Pekola, B. Karimi, G. Thomas, and D. V. Averin, Supremacy of incoherent sudden cycles, *Phys. Rev. B* **100**, 085405 (2019).

[51] S. Kamimura, K. Yoshida, Y. Tokura, and Y. Matsuzaki, Universal scaling bounds on a quantum heat current, *Phys. Rev. Lett.* **131**, 090401 (2023).

[52] A. M. Eriksson, T. Sépulcre, M. Kervinen, T. Hillmann, M. Kudra, S. Dupouy, Y. Lu, M. Khanahmadi, J. Yang, C. Castillo-Moreno, P. Delsing, and S. Gasparinetti, Universal control of a bosonic mode via drive-activated native cubic interactions, *Nature Communications* **15**, 2512 (2024).

[53] M. Müller, K. Hammerer, Y. L. Zhou, C. F. Roos, and P. Zoller, Simulating open quantum systems: from many-body interactions to stabilizer pumping, *New Journal of Physics* **13**, 085007 (2011).

[54] C. Monroe, W. C. Campbell, L.-M. Duan, Z.-X. Gong, A. V. Gorshkov, P. W. Hess, R. Islam, K. Kim, N. M. Linke, G. Pagano, P. Richerme, C. Senko, and N. Y. Yao, Programmable quantum simulations of spin systems with trapped ions, *Rev. Mod. Phys.* **93**, 025001 (2021).

[55] O. Katz, M. Cetina, and C. Monroe, n -body interactions between trapped ion qubits via spin-dependent squeezing, *Phys. Rev. Lett.* **129**, 063603 (2022).

[56] O. Katz, M. Cetina, and C. Monroe, Programmable n -body interactions with trapped ions, *PRX Quantum* **4**, 030311 (2023).